Understanding high rate behavior through low rate analog

Clive R. Siviour
Michael J. Kendall

University of Oxford
Department of Engineering Science
Parks Road
Oxford OX1 3PJ, United Kingdom

Report Date: April 2014

Final Report from 10 September 2009 to 31 January 2014

**Air Force Research Laboratory
Air Force Office of Scientific Research
European Office of Aerospace Research and Development
Unit 4515, APO AE 09421-4515**

REPORT DOCUMENTATION PAGE

Form Approved OMB No. 0704-0188

1. REPORT DATE *(DD-MM-YYYY)* 28 April 2014	2. REPORT TYPE Final Report	3. DATES COVERED *(From – To)* 10 September 2009 – 31 January 2014

4. TITLE AND SUBTITLE	5a. CONTRACT NUMBER
Understanding high rate behavior through low rate analog	**FA8655-09-1-3088**
	5b. GRANT NUMBER
	Grant 09-3088
	5c. PROGRAM ELEMENT NUMBER
	61102F

6. AUTHOR(S)	5d. PROJECT NUMBER
Clive R. Siviour **Michael J. Kendall**	
	5d. TASK NUMBER
	5e. WORK UNIT NUMBER

7. PERFORMING ORGANIZATION NAME(S) AND ADDRESS(ES) University of Oxford Department of Engineering Science Parks Road Oxford OX1 3PJ, United Kingdom	8. PERFORMING ORGANIZATION REPORT NUMBER N/A

9. SPONSORING/MONITORING AGENCY NAME(S) AND ADDRESS(ES) EOARD Unit 4515 APO AE 09421-4515	10. SPONSOR/MONITOR'S ACRONYM(S) AFRL/AFOSR/IOE (EOARD)
	11. SPONSOR/MONITOR'S REPORT NUMBER(S) **AFRL-AFOSR-UK-TR-2014-0014**

12. DISTRIBUTION/AVAILABILITY STATEMENT

Distribution A: Approved for public release; distribution is unlimited.

13. SUPPLEMENTARY NOTES

14. ABSTRACT
The research explores rate dependence in polymers. Results in the literature show that rate dependence is governed by polymer transitions. PVC was used as a model material for studying strain rate-temperature interdependence using four plasticizer levels, which modify its mechanical properties and alter the position of the transitions with respect to temperature and frequency. A methodology was then developed whereby the high rate uniaxial stress-strain response of one of the PVC compositions was simulated in low rate experiments by reducing the initial temperature, and then profiling the temperature to simulate the adiabatic heating which occurs under rapid loading. The same technique was applied to other PVC and PMMA compositions, and differences in the responses were considered. A polymer bonded sugar was tested both in compression and using the Brazilian test, and high rate data were shown to be well reproduced by low rate experiments at reduced temperature; temperature rises in these materials are very low. The experiments were supported by the development of new thermocouple and stress gauge arrangements. Although the research was mainly experimental, some complementary numerical modeling was also performed and reported.

15. SUBJECT TERMS

EOARD, high strain rate, mechanical testing, strain measurement, Hopkinson bar, polymer behavior

16. SECURITY CLASSIFICATION OF:			17. LIMITATION OF ABSTRACT	18, NUMBER OF PAGES	19a. NAME OF RESPONSIBLE PERSON Lt Col Randall Pollak
a. REPORT UNCLAS	b. ABSTRACT UNCLAS	c. THIS PAGE UNCLAS	SAR	80	19b. TELEPHONE NUMBER *(Include area code)* +44 1895 616115, DSN 314-235-6115

Standard Form 298 (Rev. 8/98)
Prescribed by ANSI Std. Z39-18

UNIVERSITY OF OXFORD

DEPARTMENT OF ENGINEERING SCIENCE

SOLID MECHANICS GROUP

Project LOW RATE	Report No. SMG 97
Title Understanding high rate behavior through low rate analog: Final Report.	

SUMMARY

This report describes research on the subject of rate dependence in polymers, performed over the past three years in the project FA8655-09-1-3088: "Understanding high rate behavior through low rate analog". The research presented was performed by Dr MJ Kendall during his doctoral studies under the supervision of Dr CR Siviour.

The research explores rate dependence in polymers. Results in the literature show that rate dependence is governed by polymer transitions. PVC is commonly plasticised, modifying its mechanical properties and changing the position of the transitions with respect to temperature and frequency. Here, PVC is used as a model material for studying strain rate – temperature interdependence in materials with four plasticiser levels.

A methodology is then developed whereby the high rate uniaxial stress-strain response of one of the PVCs is simulated in low rate experiments by reducing the initial temperature, and then profiling the temperature to simulate the adiabatic heating which occurs under rapid loading. The same technique is applied to PVC and PMMA, and differences in the responses are discussed. A polymer bonded sugar is tested in compression and using the Brazilian test, and high rate data are well reproduced by low rate experiments at reduced temperature; temperature rises in these materials are very low. The experiments were supported by the development of new thermocouple and stress gauge arrangements.

Although the research is mainly experimental, some modelling is presented in MJ Kendall's doctoral thesis.

In addition to this report, electronic copies of Dr Kendall's thesis and all papers resulting from the research have been provided.

Distribution: SMG Office (1 copy + PDF) EOARD (PDF)		**Authorised by:**	
Date	**Authors**	**Page of pages**	
28 April 2014	CR Siviour, MJ Kendall	1 of 78	

CONTENTS

Date	Authors	Page of pages
28 April 2014	CR Siviour, MJ Kendall	2 of 78

Date	Authors	Page of pages
28 April 2014	CR Siviour, MJ Kendall	3 of 78

FIGURES

Date	Authors	Page of pages
28 April 2014	CR Siviour, MJ Kendall	4 of 78

Date	Authors	Page of pages
28 April 2014	CR Siviour, MJ Kendall	5 of 78

Date	Authors	Page of pages
28 April 2014	CR Siviour, MJ Kendall	6 of 78

Date	Authors	Page of pages
28 April 2014	CR Siviour, MJ Kendall	7 of 78

Date	Authors	Page of pages
28 April 2014	CR Siviour, MJ Kendall	8 of 78

TABLES

Date	Authors	Page of pages
28 April 2014	CR Siviour, MJ Kendall	9 of 78

1 Introduction

1.1 Overview and Motivation

It has long been known that the mechanical properties of polymers are strong functions of temperature and frequency, and thus strain rate. Over the past 20 years, the rate dependence of a number of polymers has been characterised from, say, 10^{-4} to 10^4 s^{-1}, and in some cases higher. However, there are a number of experimental challenges in high rate characterisation of polymers. The most important is that, owing to their low stress wavespeed, the structural response of the specimen can affect measurements of the intrinsic material behaviour. In addition, the range of different experimental apparatus required to perform characterisation over such a range of rates can cause doubts over whether the observed effects are really an intrinsic material behaviour, or some artefact of the experimental techniques.

Over the past 10 years, time-temperature superposition has been used to address these problems, by comparing the temperature and strain rate dependencies of yield stress. This is an extension of the well-known time temperature superposition which is often applied to modulus data. Although this was initially used in the early 1970s [2], it was not applied again in this context until research by Siviour *et al.* [3] in which a linear mapping between strain rate and temperature was used to show that rate dependence in many 'engineering' polymers was affected by the lower order β transition in these materials. Since then, the mapping has been applied to a number of polymers and composites [4-10].

Having used time-temperature superposition to *understand* rate dependence in polymers, this project addressed the related question of whether it can be used to *predict* high rate behaviour. Specifically, we aimed to go beyond the usual comparisons of rate and temperature dependence of yield stress to see whether the uniaxial stress-strain response of a polymer to high rate loading can be replicated in its entirety in a low rate experiment. This would have three major uses:

1) It would further overcome the physical difficulties of high rate polymer characterisation;

2) It would provide an opportunity to better understand and measure the behaviour of polymer based composites, allowing characterisation experiments to be performed on these materials with a much wider range of diagnostic equipment, such as electron microscopy and X-ray tomography, which cannot be used at high rates.

3) The process of trying to better replicate high rate behaviour would give a better understanding of the mechanisms controlling rate dependence in polymers.

The following three research activities were undertaken:

1) Characterisation of a PVC with different amounts of plasticiser, moving the glass (α) and β transitions and therefore changing the rate and temperature dependence. Characterisation experiments were performed on materials with four different plasticiser levels, and the linear mapping proposed by Siviour was applied. The mapping worked well in three of the polymers, in which the experimental data only spanned one transition, but in one of the materials, where the data spanned two transitions, a simple modification to a two process mapping was adopted. In all cases, the mapping parameters obtained by fitting the yield stress data were similar to those obtained from DMTA experiments, giving further confidence in this technique. These data are described in sections 3.1and 3.2.

2) Experimental simulation of high rate polymer behaviour. The rate-dependent response of one of the PVC materials was very well simulated in low rate experiments by reducing the initial temperature and then increasing the temperature during the deformation, as if to simulate the adiabatic conditions prevalent in high rate loading and the conversion of mechanical work into heat. After this initial success, the technique was applied to PC and PMMA: in both of these materials it was possible to replicate the higher rate behaviour, but only by applying far lower temperature rises than actually occur in the high rate experiments. This implies that there are additional microstructural features of the response which must be investigated further. The research is described in sections 0 and 3.4. To support these activities new thermocouple arrangements were developed to enable better measurements of temperature rises in polymers, section 3.6.

3) The technique was applied to a polymer bonded sugar: a particulate composite consisting of sugar crystals in a soft rubber binder. As well as being important as a simulant for polymer bonded explosives, this was identified as a good model material for the technique. Compression experiments were performed on the binder and composite, with indirect tension (Brazilian) tests performed on the composite only. During the research it became clear that the particular PBS used was not an ideal model material: the glass transition in the HTPB binder was very low, and the temperature rises during deformation, even at high rates, were negligible. However, the reduced temperature low rate experiments were shown to faithfully replicate the high rate room temperature experiments in tension and compression. This gives confidence for the further development of the technique for in-situ materials evaluation in the future. This research is described in section 3.5. As part of this research a new stress gauge arrangement was developed for the Hopkinson bar.

1.2   Summary of Literature[1]

Most polymers exhibit time dependent mechanical behaviour, as evidenced by rate-dependent elastic moduli, yield strength and post-yield behaviour. The sensitivity to rate and temperature sensitivity is seen to change in different temperature and rate regimes, with sensitivity increasing at higher rates or lower temperatures, depending on the activation or otherwise of different molecular mobility mechanisms. In several polymers, the sensitivity is understood to increase at higher rates and/or lower temperatures because of a lack of secondary molecular mobility (β-motions), which causes increased strength and stiffness. Alternatively, the increased strength in more rubbery or elastomeric polymers is accounted for by the change in molecular mobility during the glass transition (or α-transition). The key feature is that a transition which is typically observed below room temperature is observed in high strain rate data, as the transition increases in temperature with increasing strain rate [2, 3, 11-14].

While Kolsky [15] first tested polymeric materials with the split-Hopkinson bar (SHPB) system, Chou *et al.* [16] were the first to produce a significant set of SHPB data and examine the behaviour of different polymers over a wide range of strain rates (10^{-4} s^{-1} to 10^3 s^{-1}). The authors observed an increase in strain rate sensitivity of yield stress at higher rates of strain. A temperature rise in the specimen (measured by thermocouples) was also noted at higher rates, which was credited to an adiabatic thermodynamic condition, while also linking the heat created to an increase in the amount of strain softening at high strain rates.

Bauwens-Crowet [2] is understood to be the first to describe experimentally obtained large strain behaviour and yield stress, over a wide range of temperatures and strain rates, using a time-temperature equivalence method. she produced a master curve of superposed rate and temperature dependent data for PMMA, spanning strain rates from below 10^{-4} – 10^6 s^{-1}. The curve was derived from experimental data spanning 10^{-4} – 100 s^{-1} and temperatures -20 – 100 °C. Similar research on PC was performed by Rietsch and Bouette [17], who extended the range of strain rates actually tested by using an SHPB, and observed an increase in the rate dependence of the yield stress above approximately 100 s^{-1} at room temperature. Walley and Field [14] studied several polymers, focusing on rate-dependent behaviour. The tests were conducted at strain rates ranging from 10^{-2} s^{-1} to 10^4 s^{-1}, using four different apparatus, including a direct-impact Hopkinson bar for strain rates above 10^3 s^{-1}. For a significant proportion of the polymers it was observed that yield stress increased more rapidly with increasing strain rate at higher rates. Such observations were subsequently made by a number of other authors, e.g. Al-Maliky ([18], Hamden and Swallowe [19]; however, some authors

---

[1] Note that further information about PMMA, PC and PBXs is given in the relevant sections.

Date	Authors	Page of pages
28 April 2014	CR Siviour, MJ Kendall	12 of 78

suggested that the observed response at high rate may be an artefact of testing, [20, 21], rather than an intrinsic property of the polymers under investigation. If was partly to test such a hypothesis that Siviour *et al.* [3] reintroduced the use of time-temperature equivalence as a means to interpret rate dependence in PC and PVDF. The materials were characterised over a wide range of strain rates (10^{-4} to 10^4 s^{-1}) at constant temperature (room temperature), and a wide range of temperatures (-50 to 150 °C) at constant strain rate (10^3 s^{-1}). The authors proposed an empirical formula for mapping the yield stress dependence on temperature to the dependence on strain rate, which agreed well with experimental data and comparisons in literature; results for PC are presented in Figure 1 . The formula employed a linear inter-dependence of temperature and strain rate, using a reference strain rate and reference temperature as experimental constants, as well as the experimentally determined mapping parameter *D*

$$T - T_0 = D\left(\log \frac{\dot{\varepsilon}_0}{\dot{\varepsilon}} \right) \tag{1}$$

where *D* quantifies the interaction between rate and temperature and maps from a temperature *T* to a new temperature T_0, and mapping the strain rate $\dot{\varepsilon}_0$ to a new strain rate $\dot{\varepsilon}$. For example, this mapping could be used to relate data obtained at a fixed temperature over different strain rates to data obtained at a fixed strain rate over different temperatures. The parameter *D* has been termed the temperature-strain-rate equivalence parameter by other authors who have used the formula (e.g. Furmanski *et al.* [4]), and is typically found by fitting temperature dependent and rate dependent yield data, but in principle should be obtainable from DMTA data, as demonstrated in the current project. Siviour's formula was able to capture several changes in deformation mechanisms which govern changes in yield stress, including the inflection in data which involves the glass (*α*) transition in both PC and PVDF, and the inflection which is understood as the beginning of the *β* transition in PC. It should be noted

Figure 1. Comparison of the PC variation of peak stress with temperature, and the variation of peak stress with strain rate mapped onto temperature. (Siviour et al., 2005).
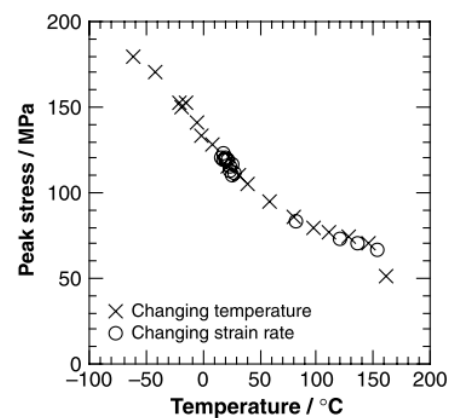
Date	Authors	Page of pages
28 April 2014	CR Siviour, MJ Kendall	13 of 78

that at the same time, Cady [22] made explicit measurements of the dependence of the glass (α) transition on strain rate and Richeton *et al.* [10] made the association between rate dependence in PC, PMMA and PAI, and the β transition,

Other authors have applied the formula to PTFE [7] and high-density polyethylene (HDPE), ultra-high molecular weight polyethylene (UHMWPE), and cross-linked polyethylene (PEX) [23]. Both found that the formula gave good agreement between their temperature dependent and rate dependent yield stress data. Williamson *et al.* [9]were able to successfully implement the linear time-temperature superposition formula to polymer bonded explosives (PBXs), a composite materials consisting of hard explosive crystals in a low modulus polymer binder. More recently, Furmanski *et al.*[4] found a linear empirical formulation of time-temperature equivalence in HDPE while investigating HDPE and UHMWPE using jump-rate compression tests to investigate isothermal high rate response with the absence of adiabatic heating.

The change from broadly isothermal to broadly adiabatic conditions as the strain rate increases is an important feature of high rate deformation, and the associated temperature rise as mechanical work is converted to heat during plastic deformation must be considered alongside the dependence on initial temperature when considering material response. Important studies involving the measurement of temperature rise in specimens during high rate deformation have been conducted by a number of authors. A notable achievement was by Chou *et al.*[16], who showed that the temperature rise in specimens inc[1]reases significantly after yield. Furthermore, Arruda et al. [24] presented visible increases in strain softening with increases in strain rate, coupled with corresponding temperature measurements using infrared detectors. Rittel [25], and later Regev and Rittel [26], used thermocouples to measure the temperature rise in specimens undergoing high rate deformation and later confirmed the accuracy of this method via infrared techniques. Additionally, Garg *et al.* [27] used infrared techniques to measure the temperature rise of PC undergoing high rate deformation. Good agreement was observed between the experimentally measured temperature rise and the 'theoretical' rise obtained by assuming that 100 % of the mechanical work is converted to heat, and adiabatic conditions prevail. Hillmansen *et al.* [28, 29]. studied plastic work being converted to heat by studying high density polyethylene (HDPE) and found, similarly, that the plastic work at large strains was approximately 100 % converted to heat. Such studies provide important background for the research presented here.

1.3 Papers and other publications

This report provides a summary of the research performed. A more detailed analysis, including discussion of constitutive modelling, is available in Dr Kendall's DPhil thesis: Experimentally Simulating High Rate Deformation of Polymers & Composites, 2013, University of Oxford. Many sections of this report are summaries of content in the thesis. The research is also described in the following journal publications:

> MJ Kendall, DR Drodge, R Froud and CR Siviour *"Strain Gage System for Measuring Very Soft Materials under High Rates of Deformation"* accepted for publication in Measurement Science and Technology

> MJ Kendall and CR Siviour *"Rate dependence of poly(vinyl chloride), the effects of plasticizer and time–temperature superposition."* Proc. R. Soc. A (2014) 20140012. http://dx.doi.org/10.1098/rspa.2014.0012

> MJ Kendall, R Froud and CR Siviour *"Novel temperature measurement method & thermodynamic investigations of amorphous polymers during high rate deformation"* Polymer (2014), doi: 10.1016/j.polymer.2014.03.058

> MJ Kendall and CR Siviour *"Experimentally simulating high-rate behaviour: rate and temperature effects in polycarbonate and PMMA"* Phil. Trans. R. Soc. A (2014) **372** 20130202 (12 pp) doi: 10.1098/rsta.2013.0202

> MJ Kendall and CR Siviour *"Experimentally simulating adiabatic conditions: Approximating high rate polymer behaviour using low rate experiments with temperature profiles"* Polymer **54** (2013) 5058-5063 doi: 10.1016/j.polymer.2013.06.049

and papers in conference proceedings:

> MJ Kendall and CR Siviour *"Strain rate and temperature dependence in PVC"* Proceedings of the 2013 SEM Conference and Exposition, Society for Experimental Mechanics

> MJ Kendall and CR Siviour *"Strain rate dependence in plasticised and un-plasticised PVC"* EPJ Web of Conferences **26**, 02009 (2012) doi: 10.1051/epjconf/20122602009.

Research was also performed which contributed to the following journal publication

> JL Jordan, JE Spowart, MJ Kendall, B Woodworth and CR Siviour *"Mechanics of particulate composites with glassy polymer binders in compression"* Phil.Trans. R. Soc. A (2014) **372** 20130215 (12 pp) doi: 10.1098/rsta.2013.0215

and one more paper has been submitted:

Date	Authors	Page of pages
28 April 2014	CR Siviour, MJ Kendall	15 of 78

MJ Kendall and CR Siviour *"Experimentally Simulating High Rate Composite Deformation in Tension & Compression: Polymer Bonded Explosive Simulant"* Submitted to International Journal of Impact Engineering

Date	Authors	Page of pages
28 April 2014	CR Siviour, MJ Kendall	16 of 78

2 Methods, Assumptions and Procedures

2.1 Introduction

Over the past 100 years, a wide range of experimental apparatus has been developed for characterising the response of materials to deformation at different strain rates, Figure 2 (see also Field *et al.* [1] and the ASM Handbook Volume 8, [30]). This chapter gives an overview of the techniques available and a more detailed description of the apparatus used in this project.

The research presented here focusses mainly on mechanical behaviour under compressive loading at applied strain rates from ca. 10^{-3} to *ca.* 10^4 s^{-1}. This range of rates may be split, broadly according to the experimental techniques used and the challenges which must be met, into quasi-static testing (10^{-3} s^{-1} to 1 s^{-1}), medium rate testing (1 s^{-1} to 100 s^{-1}), and high rate testing (500 to 10^4 s^{-1}). A thorough understanding of the behaviour of amorphous polymers within this range is required in a number of fields such as military applications, automotive, aerospace or medical devices. For quasi-static experiments, conventional servo-hydraulic and screw driven machines are typically used. Such testing machines have been available commercially since the late 19th Century, and have gone through several evolutions, moving from purely mechanical machines to sophisticated electromechanical and servo-hydraulic systems with advanced electronic control. For medium rate experiments, the main
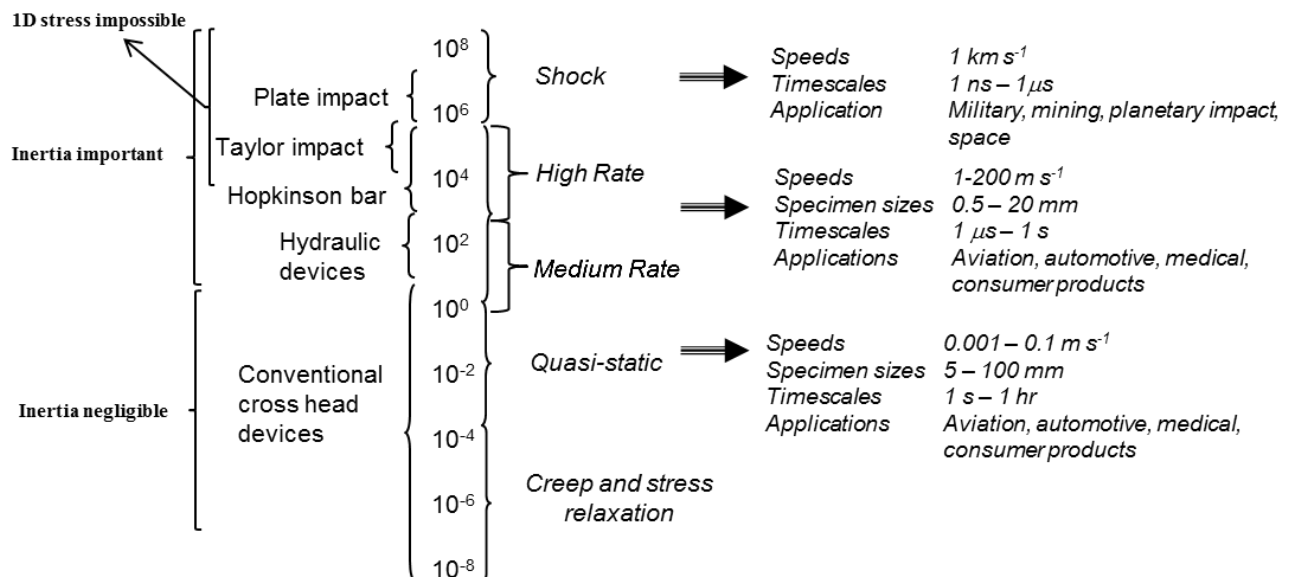
Figure 2. Approximate division of strain rate regimes (in s^{-1}), the experiments used to investigate material properties in these regimes, and selected applications. Specimen sizes are not given for plate impact, a technique that relies on wave propagation. Further information about the various techniques can be found in Field *et al.* [1].

Date	Authors	Page of pages
28 April 2014	CR Siviour, MJ Kendall	17 of 78

challenge is that the frequency at which experimental data are required is similar to the natural frequency of both the loading apparatus and the instrumentation; in addition, it is necessary to overcome the effects of the inertia of the apparatus so that high speed deformations can be applied after a very short period of acceleration. Hydraulic machines are often used; however systems based on falling weights [31], very long Hopkinson bars [32], or the 'wedge bar' [33] have also been applied successfully.

A number of techniques have been developed to measure material properties at high strain rates. These include the cam-plastometer [34, 35], and other flywheel based methods [36], the expanding ring test [18], and dropweights [31, 37]. However, the split-Hopkinson bar has now become ubiquitous for materials characterization between 500 and 10^4 s^{-1}, or even higher if miniaturized systems are used; a brief overview of the system is given below.

2.2 Quasi-static experiments

Quasi-static experiments were performed using a commercial screw-driven machine manufactured by Instron and running Bluehill 2 software. An environmental chamber with liquid nitrogen attachment was used for tests at low and high temperatures. The specimens were loaded using hardened steel anvils mounted in an alignment fixture. Standard Instron load cells were used to measure the forces applied to the specimen, whilst a clip gauge was used to measure the displacement of the anvils, from which specimen strain was calculated. Temperature control was provided by the standard thermocouple in the environmental chamber, but an additional thermocouple was attached to the loading anvils. During testing, the environmental chamber was allowed to equilibrate until the temperatures on the two thermocouples differed by less than 1 K. All temperature-time profiles were measured using the thermocouple attached to the anvil.

2.3 Medium rate experiments

Medium rate experiments were performed using an in-house hydraulic system built at Oxford University. A schematic diagram of the system is shown in Figure 3. A strain gauge based load cell with a high natural frequency has been designed, and is held against a rigid steel plate. The specimen sits below the load cell, and above a steel anvil which is connected to a hydraulically driven piston. The displacement of the specimen is measured using LVDTs, from which strain can be calculated. The piston is connected to a controller with a, limited, feedback system on which the stroke of the piston, and time taken to complete the stroke, can be specified. This allows strain rates from about 1 - 50 s^{-1} to be achieved in compressive specimens.

Date	Authors	Page of pages
28 April 2014	CR Siviour, MJ Kendall	18 of 78

2.4 High rate experiments

2.4.1 Overview

High strain rate experiments were performed using a split-Hopkinson bar system. The set-up of the test is very different from the low rate and medium rate machines described previously. In particular, instead of assuming that the apparatus is in mechanical equilibrium, propagating waves in the apparatus are used to both deform the specimen and interrogate its response. Hence the apparatus acts as a waveguide connecting a loading system (usually a gas gun), the specimen, and an instrumentation system (strain gauges). A number of excellent descriptions of the split-Hopkinson bar are available in the literature [38, 39], and a brief overview will be given here.

A schematic diagram of a compressive Hopkinson bar system is given in Figure 4. The specimen is sandwiched between two slender rods, known as the input and output bars or incident and transmitted bars, which are instrumented with strain gauges. A loading system, usually a gas gun, is used to propel a third rod, the striker bar into the input bar. This generates a stress wave which propagates down the bar to the specimen, the incident wave. At the bar-specimen interface, the change in impedance causes some of the wave to be reflected back down the input bar, and some to be transmitted to the output bar, forming the reflected and transmitted waves respectively. All three waves are measured using strain gauges on the bar surfaces. Using the three waves, and a simple 1D wave analysis, the velocities and forces at the two bar specimen interfaces, Figure 5, can be calculated from the following equations:

$$F_1 = F_I + F_R \tag{2}$$
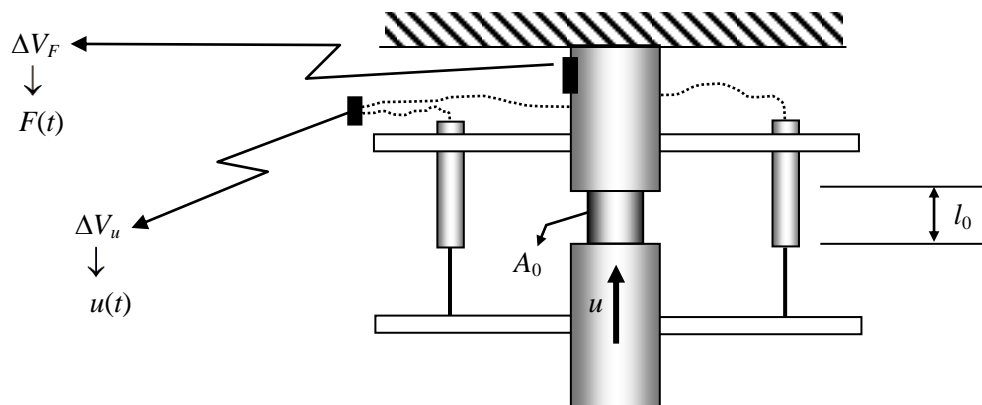
Figure 3. Schematic Diagram of the hydraulic system used for medium rate testing, indicating the load cell and LVDTs used for force and displacement measurements respectively.

Date	Authors	Page of pages
28 April 2014	CR Siviour, MJ Kendall	19 of 78

$$F_2 = F_T \tag{3}$$

$$v_1 = \frac{F_I - F_R}{\rho c A_b} \tag{4}$$

$$v_2 = \frac{F_T}{\rho c A_b} \tag{5}$$

where F_I, F_R, and F_T are the forces associated with the incident, reflected and transmitted waves, ρ, $c = \sqrt{E/\rho}$ and A_b are the density, wavespeed (E is Young's modulus) and area of the bars. Typically the same material is used for both of the bars, but it is simple to modify equations (4) and (5) if different bar materials are used.

It is usual to assume that the specimen is in stress-equilibrium during deformation, which occurs after a number of wave oscillations in the specimen. If this is the case, then the force supported by the specimen is equal to both F_1 and F_2 and the stress-strain relationship in the specimen can be calculated using the forces and bar velocities. In this project stress
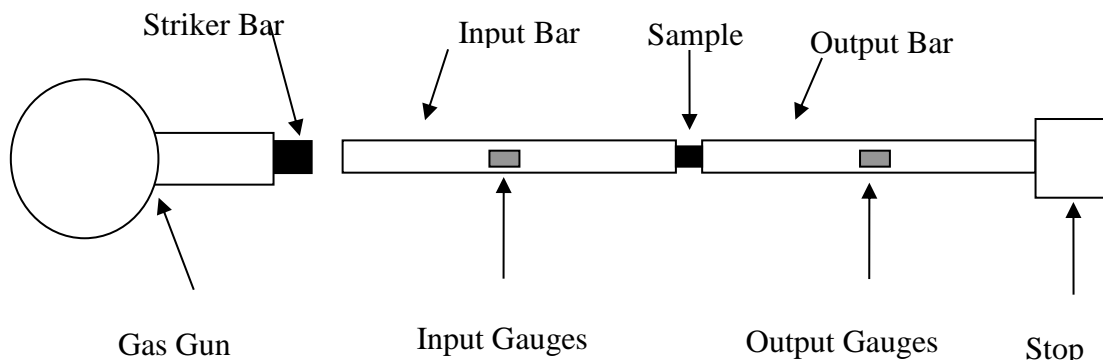
Figure 4. Schematic diagram of the split-Hopkinson pressure bar (SHPB)
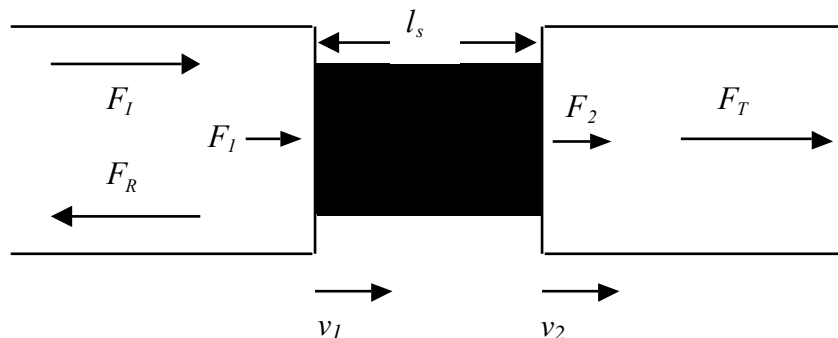
Figure 5. Forces and displacements at the two bar-specimen interfaces.

Date	Authors	Page of pages
28 April 2014	CR Siviour, MJ Kendall	20 of 78

equilibrium was confirmed in all specimens by comparing these two forces. In particular, for low wavespeed specimens, such as polymers, considerable strains can develop before equilibrium is achieved, and specimen should be designed to allow this to happen before material properties are measured from the stress-strain curves.

For completeness, the stresses and strain reported in this project are calculated using

$$\sigma(t) = \frac{F_T(t)}{A_s(t)} \tag{6}$$

$$\varepsilon(t) = \int_0^t \frac{F_I(t') - F_R(t') - F_T(t')}{\rho c A_b} \, dt' \tag{7}$$

where A_s, the area of the specimen is calculated assuming that the volume of the specimen remains constant during deformation.

2.4.2 Specific Details of Oxford SHPB

The SHPB at Oxford University consists of a 1000 mm long input bar and a 500 mm long output bar. The striker bar is 480 mm long, and all bars are 12.7 mm diameter. Both the input and output bars are instrumented with foil strain gauges, the input bar halfway along its length, and the transmitted bar 50 mm from the bar-specimen interface. This arrangement ensures long experimental durations in a physically short system, by extending the time before the transmitted wave overlaps with itself. At each 'gauge station' four gauges are used, spaced at 90° around the bar. The signal conditioning is based on a Wheatstone bridge, but slightly modified. Gauges on opposite sides of the bar are connected together and, with a balancing resistor, form a half-bridge. The two half-bridges so formed are then connected back-to back, so that in one of them a compressive strain produces a rising voltage, and in the other a falling voltage. The difference between these two signals forms the bridge output. Signals are recorded using a National Instruments data acquisition system. Each bar is statically calibrated to give a relationship between the gauge output and the force in the bar.

A number of bar materials are available; for the current project, nearly all experiments were performed using either Titanium alloy (Ti64) or Magnesium alloy (AZM) bars. Both of these are low stiffness, high strength materials which give large gauge signals even when testing soft polymers, but are strong enough not to yield at the impact speeds required for the higher strain rate experiments.

2.5 Specimen design and lubrication

2.5.1 Specimen size

All specimens were right cylinders, typically with lengths and diameters of the order 5 to 10 mm, details are given in the appropriate chapters. For most of the studies the same specimen dimensions was used in all experiments, and these were chosen to satisfy the specific requirements of high rate testing, mainly equilibrium and inertia as discussed below. This meant that the specimens were not optimised for low strain rate experiments, and in particular are too short to give accurate modulus values. However, since the time taken to reach equilibrium in the high rate experiments means that modulus comparisons across strain rates cannot be performed, and indeed the available materials meant that longer specimens could not, in most cases, be manufactured, this did not affect the ability to address the research questions posed. Further discussion of specimen sizes in experimental programmes across a wide range of strain rates is given in [40].

When designing specimens for high rate experiments, two key factors must be taken into account. Firstly, the specimens must be short enough to allow stress equilibrium to occur in a reasonable timescale. Although stress equilibrium was confirmed in the experiments performed, a reasonable rule of thumb for specimen *design* is that three wave reverberations are required along the specimen length. For polymers this limits the specimen length to about 5 mm, less for rubbers.

The second consideration is specimen inertia. When the specimen is loaded, some force is required to overcome the intrinsic material strength, whilst some is required to accelerate the material to the high deformation speeds, in both the axial and radial directions. Gorham [41] calculated that the pressure measured on the output bar is given by

$$P_2 = \sigma_y - \rho\left(\frac{r^2}{8} - \frac{h^2}{6}\right)\ddot{\varepsilon} + \rho\left(\frac{r^2}{16} - \frac{h^2}{6}\right)\dot{\varepsilon}^2 - \frac{\rho h \dot{v}}{2} \tag{8}$$

where σ_y is the intrinsic material strength, r and h the specimen radius and height respectively and $\dot{v}$ the velocity of the output bar. This equation, which has been derived for an incompressible specimen, can be used as a guide to specimen design, ensuring that the inertial contribution is significantly smaller than the actual material strength.

2.5.2 Lubrication

Lubrication is an important consideration in all compression experiments, but especially in high rate testing of polymers, where the low sound speeds mean that short specimens are required, and the low strengths often encourage the use of specimens with large diameters.

Date	Authors	Page of pages
28 April 2014	CR Siviour, MJ Kendall	22 of 78

Hence, the aspect ratio of the specimen is small (*h/r*), which can lead to significant frictional effects. If there is excessive friction, a barrelling effect is observed, causing stress inhomogeneity and an increase in the measured specimen strength: such tests are not valid for the measurement of the bulk properties of a material. Studies of different lubricants, (e.g. (Trautmann *et al.*[42] and Okereke *et al.* [43]) have shown that paraffin wax is a suitable lubricant at all rates and temperatures explored in the current project, and hence this is used for all experiments described in this report.

2.6   Other experimental techniques

2.6.1   DMTA

Dynamic mechanical and thermal analysis (DMTA) machines apply oscillating displacements with systematic variations of temperature (e.g. -100 °C to 200°C) and/or frequency (up to approximately 100 Hz). By measuring force and displacement as functions of time, with particular reference to the phase of these quantities, it is possible to calculate the complex modulus and loss tangent of the specimen material. Commonly used configurations include single or dual cantilever, tension and compression. In this project, DMTA was regarded as a 'black-box' tool, to provide supporting date for the rate dependent mechanical characterisation. Experiments were performed on a TA instruments Q800 machine in a dual cantilever configuration, and data reported were calculated by the TA instruments software. Amongst other data, the software provides outputs of storage modulus and loss tangent as a function of temperature at different frequencies, which are reported for the materials in this report.

For comparison to other data, the frequencies from the DMTA experiments must be converted to strain rates. This was done using the following approximation, which is commonly applied in the literature (e.g. [12])

$$\dot{\varepsilon} \approx \frac{\Delta\varepsilon}{\Delta t} = \frac{\varepsilon_0}{1/4f} = 4f\varepsilon_0 \tag{9}$$

where ε_0 is the strain amplitude reported by the DMTA machine, and f the oscillation frequency. Specimen sizes were typically $50 \times 10 \times 2 - 5$ mm.

2.6.2   Brazilian Tests

The Brazilian test (or indirect tension test) is commonly used for characterising brittle materials, such as concrete or ceramics, and was, in this project, used to perform tensile tests on polymer bonded sugar, in the same fashion as Rae *et al.*[44] and others. In this test, a thin

Date	Authors	Page of pages
28 April 2014	CR Siviour, MJ Kendall	23 of 78

disk of material is compressed along a diameter. This causes a tensile strain to develop in the centre of the disk, perpendicular to the loading direction, an example of a tensile failure in such a test is given in Figure 6. Advantages of this test compared to dog-bone tensile specimens are simplified specimen preparation, a much reduced dependence of the measured strength on surface finish and alignment, and much smaller specimen sizes, important when only small quantities of material are available or if there are safety concerns. For these reasons, the Brazilian test is often used for characterisation of Polymer Bonded Explosives (PBXs).

The Brazilian test configuration used in the current project is based on the research of Awaji and Sato [45], who introduced the use of curves anvils to reduce stress concentrations at the contacts between the anvil and specimen. The authors derived an equation for calculating the tensile stress in the specimen from the applied compressive load:

$$\sigma = \frac{2P}{\pi D_s t_s}\left(1 - \left(\frac{b}{R_s}\right)^2\right) \tag{10}$$

where P is the applied load, D_s and t_s the diameter and thickness of the specimen respectively, R_s the radius of the specimen, and b the contact width of the specimen with the anvils. In addition, it was shown by Awaji and Sato that if the ratio b/R_s is greater than 0.27, then the tensile strength of the specimen is independent of b/R_s. Following the examples of, e.g. Rae *et al.*, 2002; Williamson *et al.*, 2009 and Grantham *et al.*, 2004, [9, 46, 47], Digital image correlation (DIC) was used to measure displacements and hence calculate strains on the specimen surface during testing. Images were taken with a Nikon D3100 DSLR camera in quasi-static experiments and a Photron SA5 high speed camera in Hopkinson bar experiments. In this case, it was established that the natural patter in the specimens was sufficient to provide the random pattern required for DIC, and analysis was performed using commercial software (DaVis 2D strain analysis software from LaVision).
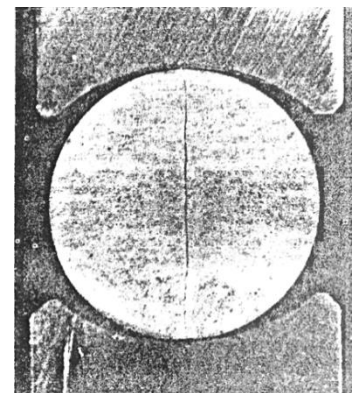
Figure 6. Brazilian test configuration where the tensile failure is seen at the center of the cylindrical specimen (marble) created from the compressive loading of curved anvils (Awaji & Sato, 1978)

Date	Authors	Page of pages
28 April 2014	CR Siviour, MJ Kendall	24 of 78

3 Results and discussion

3.1 PVC – Experimental characterisation and effect of plasticiser

3.1.1 Materials

A discussed in the Introduction, most polymers exhibit time dependent mechanical behaviour, as evidenced by rate-dependent elastic moduli, yield strength and post-yield behaviour, which is governed by the shifts of the α and β transitions with strain rate. The capability to alter these transitions through the incorporation of additives such as plasticizers offers an opportunity to better understand these effects. In many applications in which poly(vinyl chloride) (PVC, Figure 7(a)) is used, it is blended with a plasticizer based on an phthalate ester compound, such as diisononyl phthalate (DINP) (Figure 7(b)). The plasticizer is used to enhance ductility and decrease properties such as the yield stress and stiffness. By changing the amount of plasticiser, the temperature- and rate-dependence are modified. In the context of the current research, the importance of this is that it allows one to better analyse the mechanisms that govern these dependencies, offering insight into the interplay between temperature and rate dependence of polymers. Selected properties of unplasticized PVC and plasticized PVC are listed in Table 1.

In this section a combination of experimental and analytical research is presented to establish the interplay between rate- and temperature- dependence in four different PVC materials, which were manufactured and supplied by Solvin. As outlined in Table 2, the four PVCs examined range from an unplasticized form, 'PVC', to the most plasticized form, 'PPVC-6', with 60 wt% plasticizer content. DINP was used as the plasticizing agent. The PVC came as pressed plates with dimensions of 11.5 x 20 cm and a thickness of 2.5 mm. Specimens were machined from these plates.

(a)   (b)
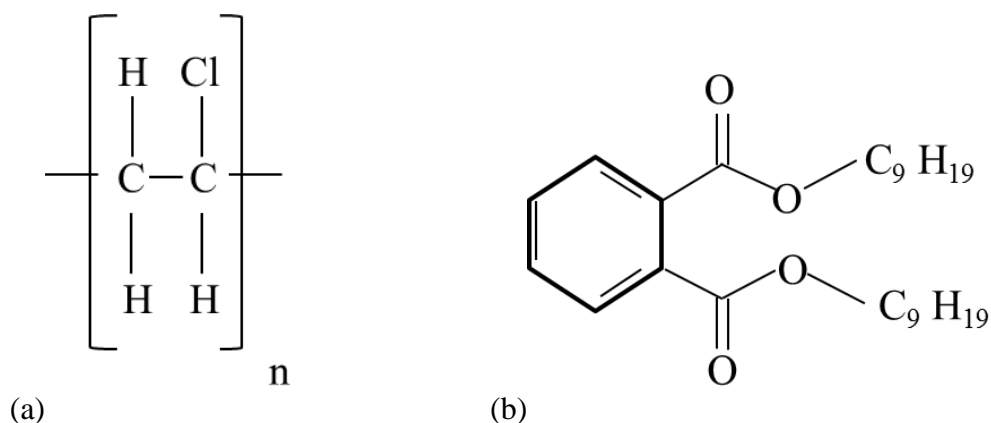
Figure 7. Chemical structure of (a) poly(vinyl chloride) and (b) diisononyl phthalate.

Date	Authors	Page of pages
28 April 2014	CR Siviour, MJ Kendall	25 of 78

Table 1. Selected properties of unplasticized PVC and plasticized PVC [13, 48].

Property	Unplasticized PVC	Plasticized PVC
Density [g·m^{-3}]	1.3–1.45	1.1–1.35
Tensile strength at yield [MPa]	31–60	10–25
Young's modulus [MPa]	2500	250
Glass Transition Temperature[°C]	82.4	-20
Melting Point [°C]	100-260	40-50
Thermal conductivity [W·m^{-1}·K^{-1}]	0.14–0.28	0.14–0.17

Table 2. The four PVC materials used in the reported research.

Resin	Label in text	Amount of Plasticizer [wt%]	Measured Density [g·cm^{-3}]
DGA166-09	PVC	0	1.429
264-01PC	PPVC-2	20	1.317
264-03PC	PPVC-4	40	1.263
264-05PC	PPVC-6	60	1.214

3.1.2 Compression Experiments: Specimen Geometry

All specimens were right circular cylinders with the axis of the specimen perpendicular to the plane of the plate. Previous work has suggested that length-to-diameter ratios of 1:2 or less are required when testing of low-impedance materials at high rates in order to achieve equilibrium. This ratio provides a good compromise between the effects of axial, radial, and tangential inertia in the specimen, and wave propagation time [41, 49].

The specimen length was fixed by the 2.5 mm thickness of the plates, and diameters of 5 mm and 8 mm were initially used. During the initial testing of PVC and PPVC-6, both specimen sizes were used at all rates tested in order to allow

for a more straightforward comparison between rates. During SHPB testing, a thin layer of petroleum jelly was used on the impact side of the incident bar for pulse shaping the incident pulse; this reduces the characteristic high-frequency Pochhammer-Chree oscillations associated with the propagation of the stress pulse, and increases the rise time of the incident pulse, which assists in establishing stress equilibrium [10]. Dynamic equilibrium, defined as the force on the interface between the incident bar and the specimen ($F_I + F_R$) being equal to the force at the interface between the specimen and the output bar (F_T), was achieved before yield in all tests.

During low rate tests the two specimen sizes demonstrated identical material responses to deformation, Figure 8(a). In high rate tests, however, ringing was observed in the results from the 8 mm specimens as compared to the 5 mm specimens, Figure 8(b). This is due to increased radial inertia in the 8 mm specimen, use of which was therefore discontinued.

(a)   (b)
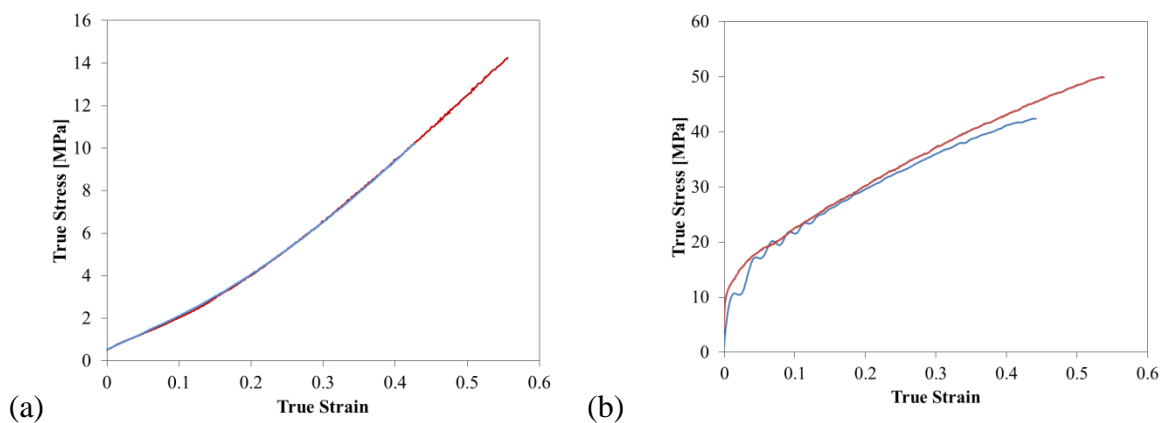
Figure 8. Comparison of data from low, 10^{-2} s^{-1}, (a) and high, 3000 s^{-1}, (b) rate experiments on PPVC6, comparing 5 mm (red) and 8 mm (blue) diameter specimens. Note the ringing on the curve from the 8 mm specimen in (b).

Date	Authors	Page of pages
28 April 2014	CR Siviour, MJ Kendall	27 of 78

Table 3. Inertial contributions of each material compared to the room temperature flow stresses at the highest rates tested.

Material	Room Temperature Flow Stress [MPa]	At strain rate [s^{-1}]	Inertial Contribution [kPa]
PVC	155	6300	100
PPVC-2	140	7550	68
PPVC-4	65	14000	24
PPVC-6	26	13500	16

A further consideration in specimen design for high strain rate experiments is inertia. Inertial contributions and room temperature flow stresses for each material, calculated using equation (8) are compared in Table 3. It is shown that inertial contributions are negligible compared to the room temperature strength of each material tested.

3.1.3 Compression Experiments: Experimental overview

Uniaxial compression tests were performed over strain rates ranging from 10^{-3} s^{-1} to 14000 s^{-1}. Tests at 10^{-3}, 10^{-2}, and 10^{-1} s^{-1} were performed using an Instron testing machine. Force measurements were taken from the load cell and displacement measurements from a clip gage extensometer attached to the loading platens. Quasi-static experiments were conducted over the temperature range -115 to 100 °C using a standard Instron environmental chamber. Temperature readings from the environmental chamber were confirmed by the use of thermocouples attached to the platens adjacent to the specimen-platen interface.

Experiments at rates ranging from 1 s^{-1} to 100 s^{-1} were conducted on the custom-built hydraulic load frame described in chapter 2. Linear variable differential transformers (LVDTs) were used to measure the displacements of the anvils, and a strain gauge based load cell measured the force supported by the specimen. These data were used to calculate the stress-strain relationship in the sample.

High rate tests were performed from 550 s^{-1} to 14000 s^{-1} on a split-Hopkinson pressure bar (SHPB) apparatus using magnesium alloy (AZM), titanium (Ti-6Al-4V), and steel bars. The striker bar, incident bar, and transmitted bars all had diameters 12.7 mm, with lengths of 0.5 m, 1.0 m, and 0.5 m, respectively. The strain gauges were placed 0.5 m from the specimen-bar interface on the incident bar and 50 mm from the specimen-bar interface on the transmitted bar. The standard analysis described in chapter 2 was used to calculate stress-strain curves, and dynamic equilibrium was confirmed after each test by calculating force-time profiles for both specimen-bar interfaces.

Date	Authors	Page of pages
28 April 2014	CR Siviour, MJ Kendall	28 of 78

3.1.4 Compression Experiments: Results and Analysis

Figure 9 to Figure 16 summarise the rate dependent response at 20°C and temperature dependent response at 10^{-2} s^{-1} of each material tested. These data are parameterised by the dependence of yield stress on strain rate and temperature, where the yield stress is recognized as the peak stress that the polymer reaches around yield: the intrinsic yield described by Bowden [2]. For the rubbery materials, for which there is either no yield, or it is indistinct, the true stress at 5% true strain is instead plotted.

The response of unplasticised PVC (Figure 9(a), Figure 10(a)) to compression at different strain rates and temperatures is the same as observed in previous literature. Its glassy polymer response is characterized by initial linear visco-elasticity followed by yield, then strain softening, and subsequently strain hardening. Literature data for the rate-dependence of yield is typically described as approximately linear (in log strain rate) in the low to medium rate regime, before transitioning to a second (and steeper) linear dependence in the high rate regime. In the data presented here, Figure 9(b), a similar increase in rate dependence is observed as the strain rate increases, although this may be described more as a smooth transition rather than a strictly bilinear dependence. This is discussed further below, but is due to the effect of the β transition, i.e. the inability of β-motions to occur on the timescale of the experiment, at the higher strain rates.

The behaviour of PPVC-2 in uniaxial compression is summarized in Figure 11(a) and Figure 12(a). The addition of plasticizer causes an increase in strain softening post yield. A further important observation is that the low rate data show significant strain hardening at

(a)   (b)
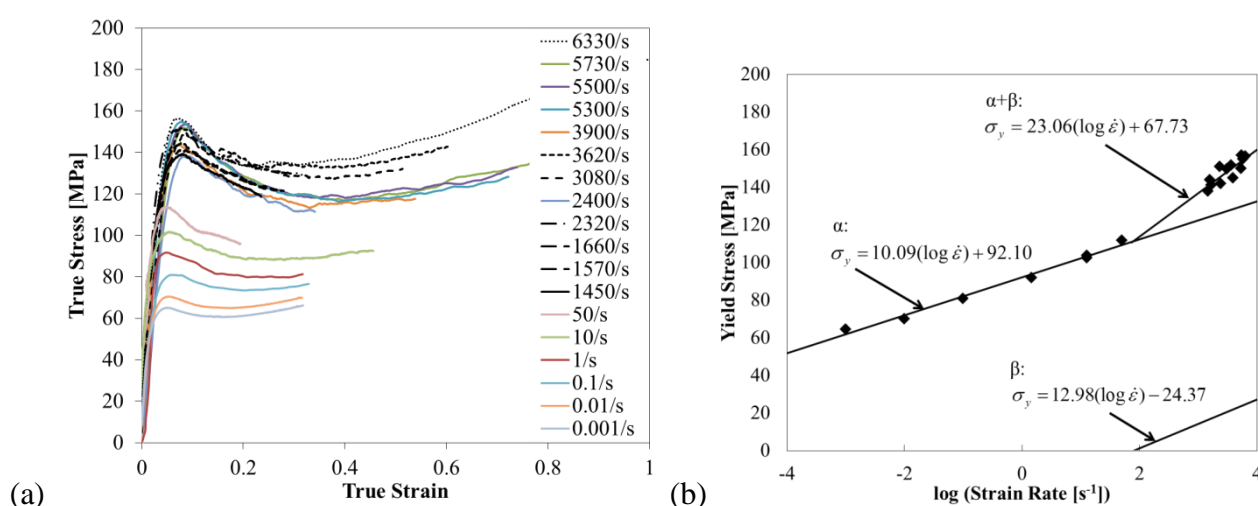
Figure 9. Representative behaviour of PVC. (a) True stress-true strain response in uniaxial compression over all rates tested at 20 °C; (b) True yield stress as a function of strain rate.

Date	Authors	Page of pages
28 April 2014	CR Siviour, MJ Kendall	29 of 78
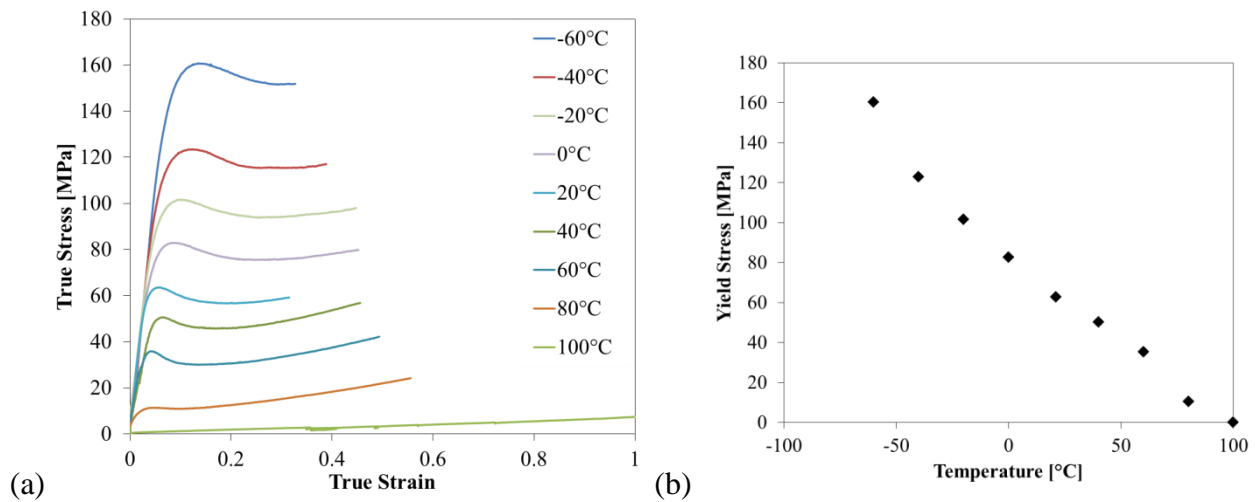
Figure 10. Representative behaviour of PVC. (a) True stress-true strain response in uniaxial compression over all temperatures tested at 10^{-2} s^{-1}; (b) True yield stress as a function of temperature.
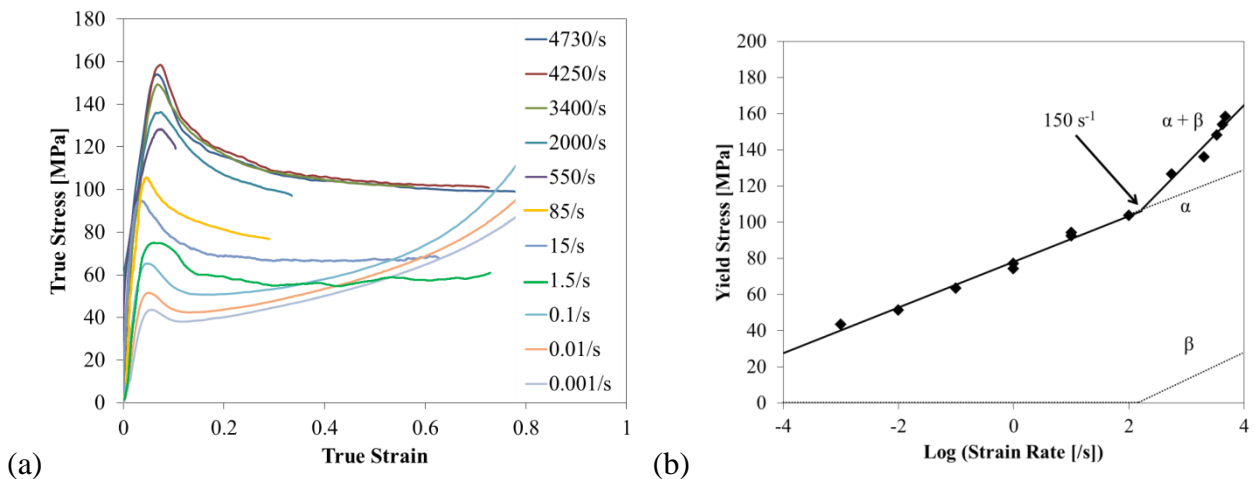
Figure 11. Representative behaviour of PPVC-2. (a) True stress-true strain response in uni-axial compression over all rates tested at 20 °C; (b) True yield stress as a function of strain rate.

larger strains, which is not observed at strain rates above c.a. 1.5 s^{-1}. This observation is explored further in section 0. The dependence of yield stress on strain rate and temperature is shown in in Figure 11(b) and Figure 12(b). The rate dependent data show a transition in material response at approximately 150 s^{-1}, again owing to the effect of the β transition.
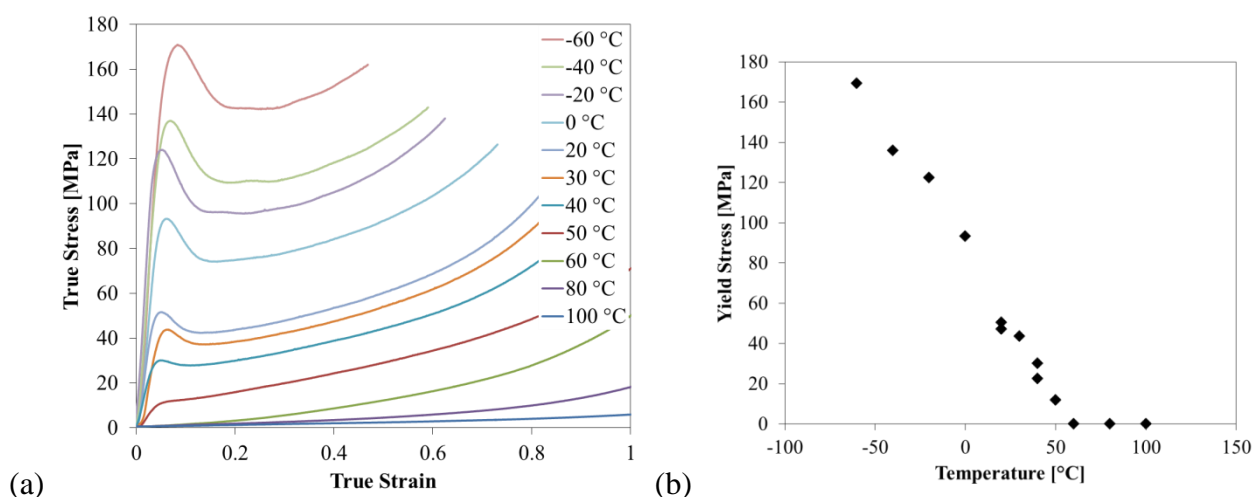
Figure 12. Representative behaviour of PPVC-2. (a) True stress-true strain response in uniaxial compression over all temperatures tested at 10^{-2} s^{-1}; (b) True yield stress as a function of temperature.

PPVC-4 and PPVC-6 present similar responses to each other; both have glass transition temperatures well below room temperature. The glass transition of PPVC-4 is observed in the temperature dependent yield data Figure 14 at approximately 0 °C, while the glass transition of PPVC 6 is at -30 °C, Figure 16. Both of these transition temperatures have been confirmed by DMTA data, discussed further below. These transitions are also visible in the stress-strain responses in both the temperature dependent and rate dependent data.

Examining the stress-strain response of both materials, in Figure 13 to Figure 16, as strain rate increases, or temperature decreases, the behaviours change from rubbery to 'leathery' to glassy as the effect of the glass transition (which has been moved below room temperature by the plasticiser) comes into play. The effect of the increased plasticiser content in PPVC-6 relative to PPVC-4 is to reduce the temperature of the glass transition, and therefore increase the strain rate required before this transition affects the stress-strain response. Hence, behaviour observed at the highest rates in PPVC-6 is seen at lower rates in PPVC-4. It is, however, worth noting the similarity of the PPVC-6 stress-strain response at -20 °C to that at 2000 s^{-1}, highlighting the interplay between strain rate and temperature. Conversely, the rate dependent response of PPVC-4 presents strain hardening after yield, which is not present in the temperature dependent response up to the plastic strain tested. Thus, although rate – temperature equivalence can help to understand the mechanical response of the polymer, it does not give the full picture.

Date	Authors	Page of pages
28 April 2014	CR Siviour, MJ Kendall	31 of 78
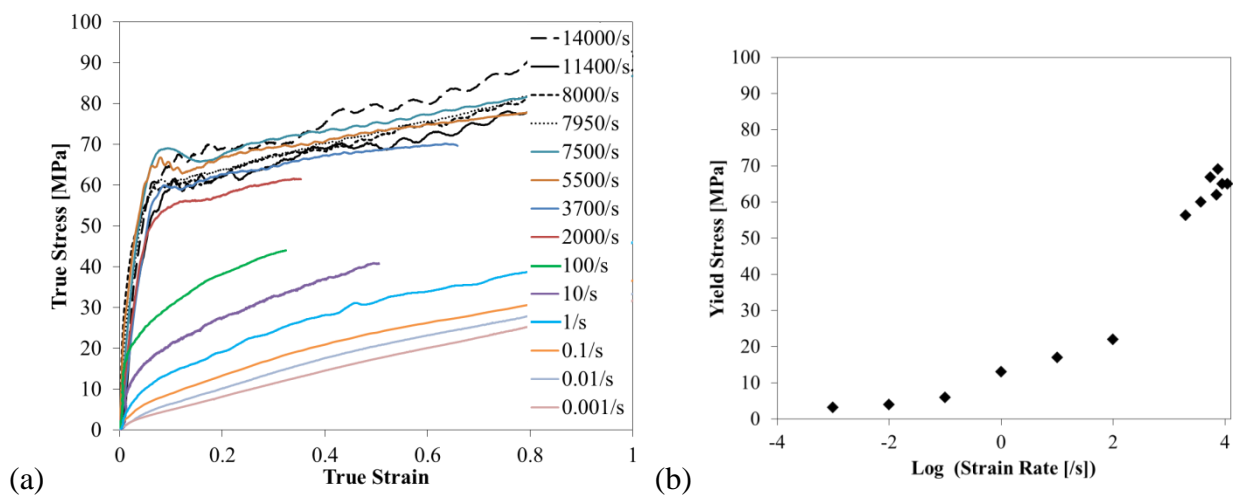
Figure 13. Representative behaviour of PPVC-4. (a) True stress-true strain response in uni-axial compression at 20 °C; (b) True yield stress as a function of strain rate.
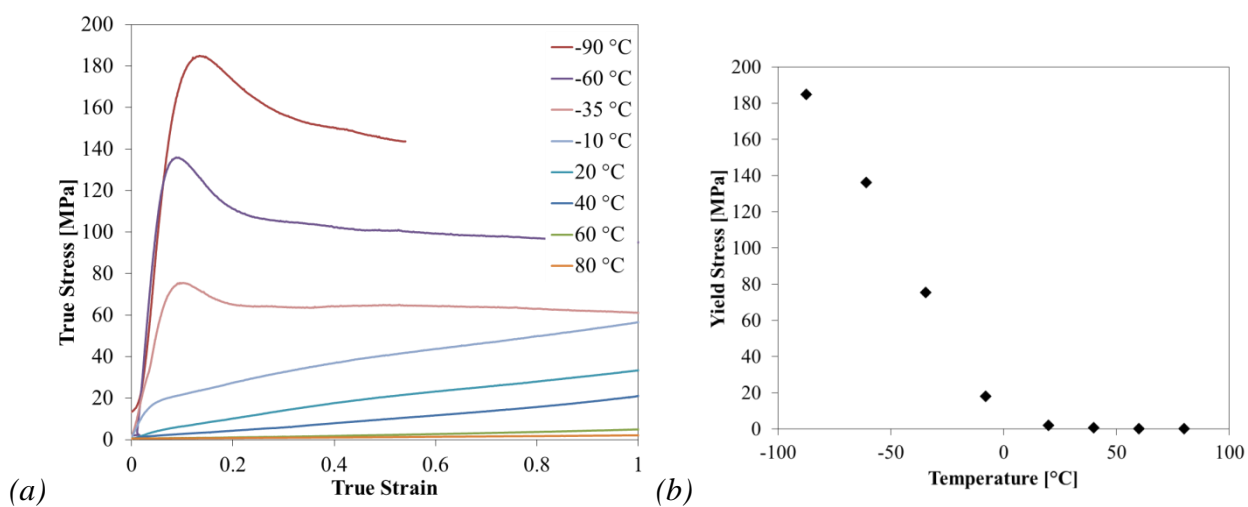
Figure 14. Representative behavior of PPVC-4. (a) True stress-true strain response in uniaxial compression over all temperatures tested at 10^{-2} s^{-1}; (b) True yield stress as a function of temperature.

Date	Authors	Page of pages
28 April 2014	CR Siviour, MJ Kendall	32 of 78
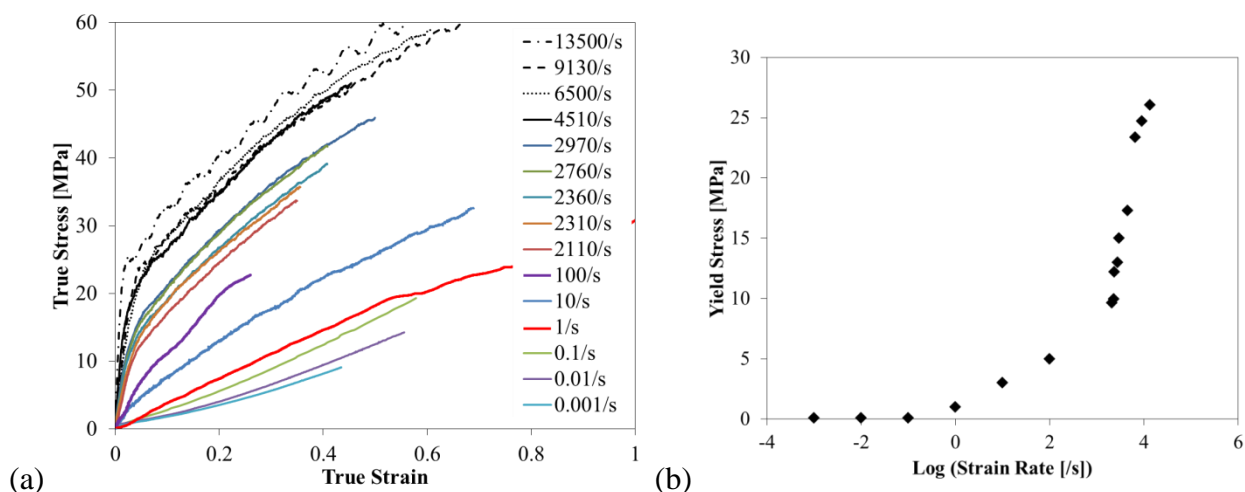
Figure 15. Representative behaviour of PPVC-6. (a) True stress-true strain response in uni-axial compression over all rates tested at 20 °C; (b) True yield stress as a function of strain rate.
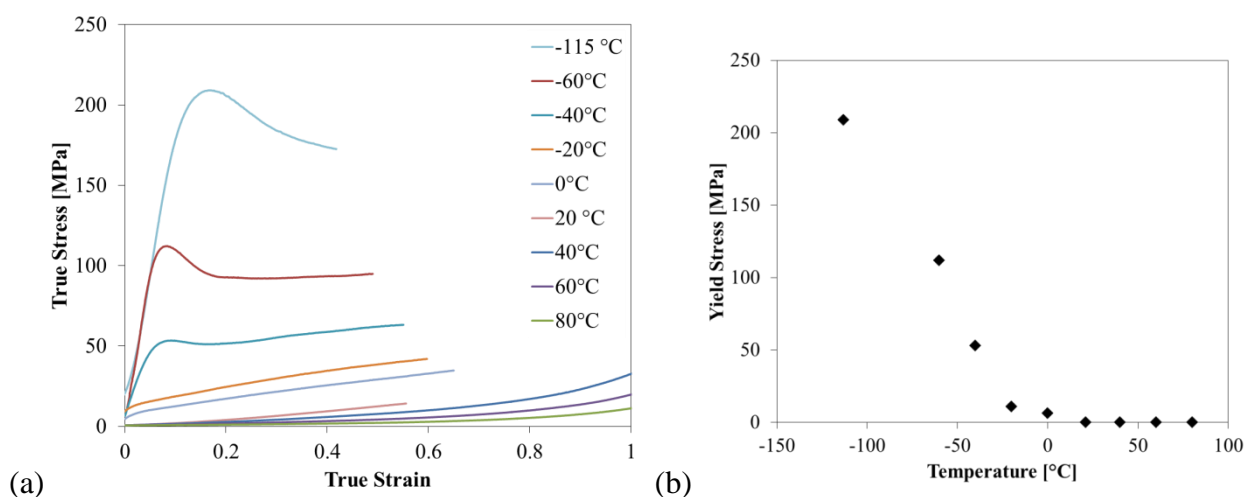
Figure 16. Representative behaviour of PPVC-6. (a) True stress-true strain response in uniaxial compression over all temperatures tested at 10^{-2} s^{-1}; (b) True yield stress as a function of temperature.

3.1.5 DMTA Data

DMTA experiments were performed on a TA Instruments Q800 DMTA. The rectangular specimens had dimensions of 2.5 mm height, 10 mm width, and 35 mm length, and were used in the dual-cantilever mode of the DMTA machine with an amplitude of 20 μm. Tests were performed at temperatures ranging from -100 to 100°C with an additional test on PPVC-6 from -150 to 30 °C to investigate the shift of the β transition with the increase in plasticizer. Testing was conducted at frequencies of 1, 10, and 100 Hz, with the exception of the unplasticized PVC material (0.1, 1, and 10 Hz).

Characteristic storage and loss modulus curves for all tested frequencies are shown in Figure 17 to Figure 21. The test frequencies are converted to their approximate strain rates using equation (9). The PVC loss modulus, Figure 17, has two large peaks corresponding to the α and β transitions. PVC has an α transition centered at 82 °C which agrees with literature measurements (e.g. Table 1 and [50]). Subsequent figures show the α transition shifting to lower temperatures with increasing amounts of plasticizer. PPVC-2 has an α-peak located at 45 °C, PPVC-4 at 0 °C, and PPVC-6 at -30 °C. The loss modulus peak corresponding to the α transition also broadens with the addition of plasticizer: for PVC it spans 40 °C, while PPVC-2 spans approximately 80 °C, and PPVC-4 and -6 span 100 °C.

The loss modulus peak relating to the β transition is at approximately -45 °C in the unplasticised PVC, and overlaps slightly with the peak corresponding to the glass transition, although there is enough spacing for the effect of the two transitions to be distinguished in the storage modulus response. For the plasticised materials, there is a slight bend approaching -100 °C which was thought to correspond to the beginning of the β transition. This was confirmed by an additional test on PPVC-6 over a temperature range from -150 to 30 °C.

Figure 17. PVC elastic modulus (solid lines) and loss modulus (dashed lines) curves at 0.035 s^{-1} (1 Hz – green), 0.35 s^{-1} (10 Hz – blue), and 3.5 s^{-1} (100 Hz – red). β transitions and α transitions are centred respectively at approximately -45 °C and 82 °C.
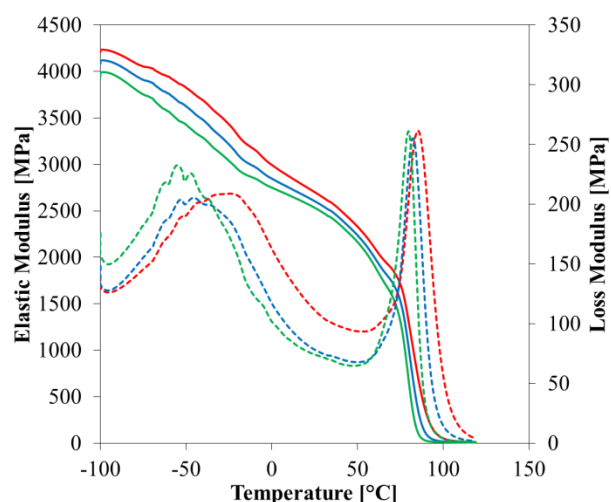
Date	Authors	Page of pages
28 April 2014	CR Siviour, MJ Kendall	34 of 78

Figure 18. PPVC-2 elastic modulus (solid lines) and loss modulus (dashed lines) curves at 0.035 s^{-1} (1 Hz – green), 0.35 s^{-1} (10 Hz – blue), and 3.5 s^{-1} (100 Hz – red). The α transition is centred at ~ 45 °C.
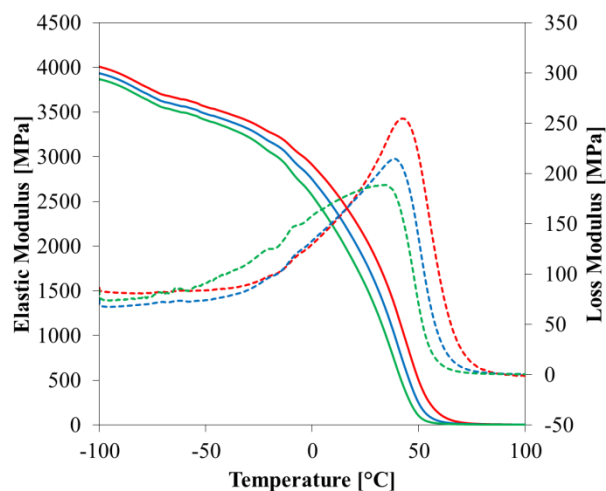
Figure 19. PPVC-4 elastic modulus (solid lines) and loss modulus (dashed lines) curves at 0.035 s^{-1} (1 Hz – green), 0.35 s^{-1} (10 Hz – blue), and 3.5 s^{-1} (100 Hz – red). The α transition is centred at ~ 0 °C.
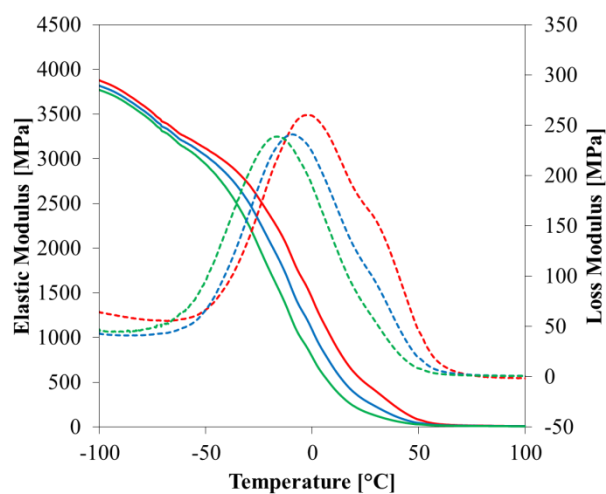
Figure 20. PPVC-6 elastic modulus (solid lines) and loss modulus (dashed lines) curves at 0.035 s^{-1} (1 Hz – green), 0.35 s^{-1} (10 Hz – blue), and 3.5 s^{-1} (100 Hz – red). The *α* transition is centered at approx.-imately -30 °C.
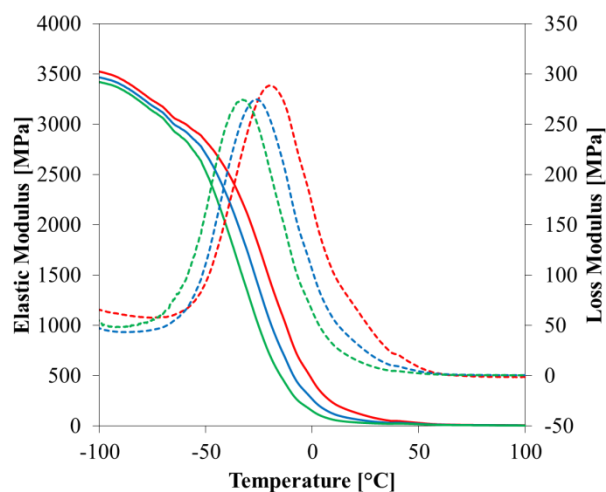
Date	Authors	Page of pages
28 April 2014	CR Siviour, MJ Kendall	35 of 78

Figure 21. PPVC-6 elastic modulus and loss modulus curves at 0.035 s^{-1} (1 Hz – green), 0.35 s^{-1} (10 Hz – blue), and 3.5 s^{-1} (100 Hz – red). β transitions and α transitions are centered respectively at approximately -150 °C and -30 °C.
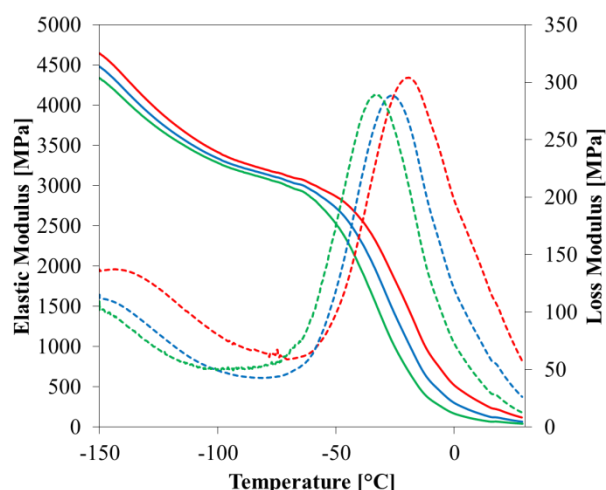
3.1.6 Comparison of DMTA and Compressive Results

Figure 22 presents a comparison of the temperature dependence of the quasi-static yield stress and the DMTA storage modulus. These data show the similarities between the increases in elastic modulus and yield stress with decreasing temperature. This will now be explored further for the unplasticised PVC as a prelude to the more detailed discussion of time-temperature equivalence in the next section. From the DMTA data, it is possible to obtain the frequency, or rate, dependence of the α and β transitions and to extrapolate these dependencies to find the strain rate at which the β transition occurs at room temperature. Above, this rate, the strength of the polymer is expected to increase because β motions are no longer able to occur on the allowed timescales. This extrapolation, for unplasticised PVC, is shown in Figure 23, and gives a strain rate of about 100 s^{-1}, which agrees well with the change of gradient of yield stress against log(strain rate) in Figure 9.

Date	Authors	Page of pages
28 April 2014	CR Siviour, MJ Kendall	36 of 78
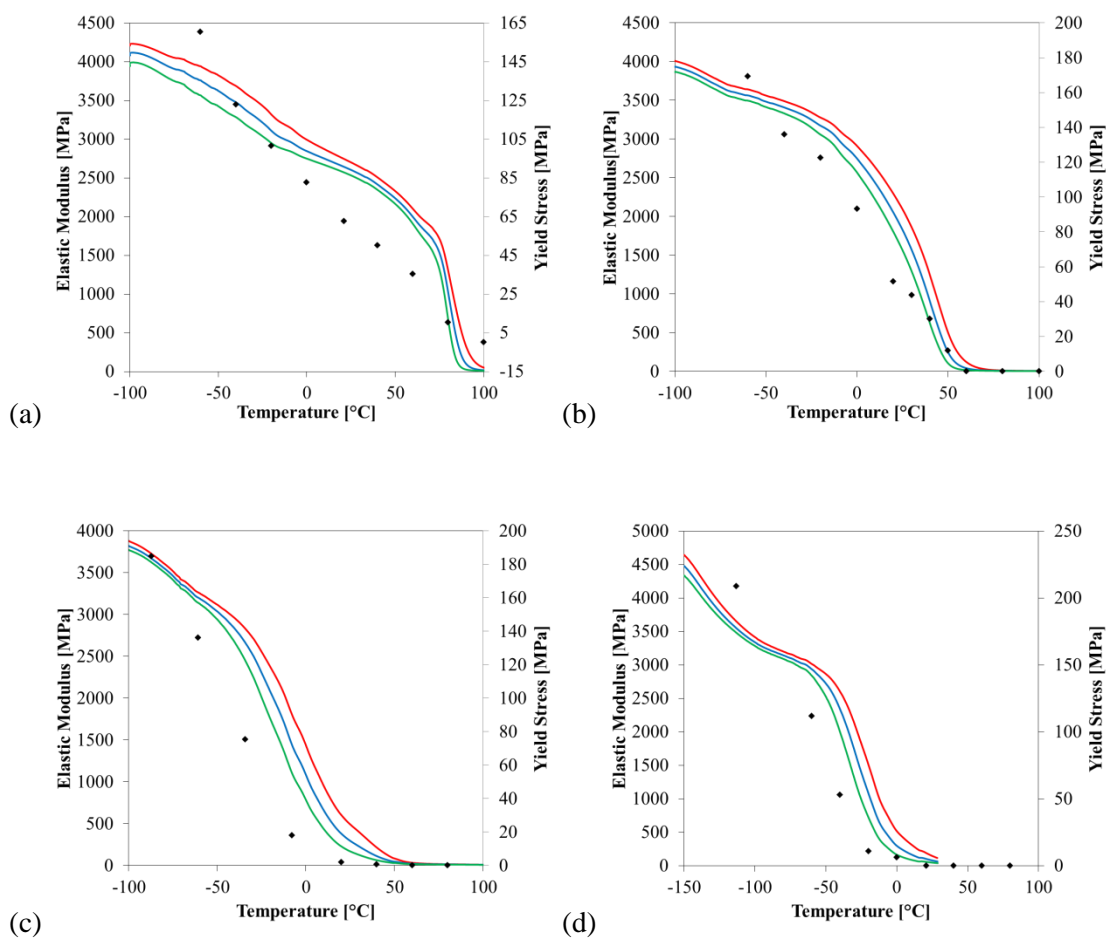
Figure 22. DMTA data for PVC (a), PPVC-2 (b), PPVC-4 (c), and PPVC-6 (d) at 0.035 s^{-1} (1 Hz – green), 0.35 s^{-1} (10 Hz – blue), and 3.5 s^{-1} (100 Hz – red) with yield stress data at 10^{-2} s^{-1} superposed.
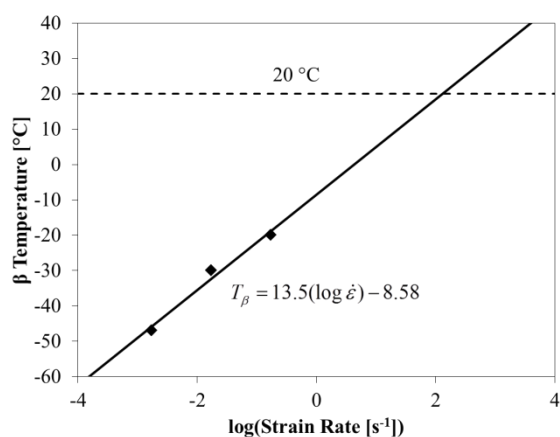
Figure 23. Dependence of the β transition temperature on strain rate in unplasticised PVC.

$$T_\beta = 13.5(\log \dot\varepsilon) - 8.58$$

Date	Authors	Page of pages
28 April 2014	CR Siviour, MJ Kendall	37 of 78

3.2 PVC – Time-temperature equivalence

3.2.1 Background

The application of time-temperature superposition to the yield stress of various polymers is discussed in Section 1. In particular, this report will concentrate on the application of the linear mapping between temperature and strain rate proposed by Siviour (equation (1)) This has been shown to capture the relationship between rate and temperature dependence in a number of polymers, giving a better understanding of the underlying processes that govern the rate dependence (for a more detailed discussion of the applicability of this equation see [4] and MJ Kendall's thesis). Here, it will be shown that this equation works well for PVC, PPVC-4 and PPVC-6, in which only one process (β for PVC and α for PPVC-4 and PPVC-6) affects the rate and temperature dependence over the range of rates and temperatures examined; however, for PPVC-2, both the α and β transitions occur in the tested range and therefore a small modification to the equation is required.

3.2.2 Results and discussion

Results from the linear mapping of temperature to strain rate are shown for each of the four PVC materials in Figure 24 – Figure 27. All graphs are shown as functions of strain rate, however they could equivalently be presented in temperature. Shift factors were chosen to give the best fit between the two data sets. The figures show that good agreement can be obtained for three of the materials, but not for PPVC-2, which was therefore investigated further. Firstly, a further set of DMTA data were obtained going down to -150 °C, the lower limit of the DMTA machine. These data show a β transition in the material at low temperature. Hence, it is possible that both the α and β transitions occur in the span of experiments reported here, and further investigation into the shift of these transitions was performed.

Figure 24. PVC: Result from mapping yield stress as a function of temperature (squares) onto strain rate, compared to experimental values of yield stress as a function of strain rate (triangles). The mapping parameter was D = 13.5 °C/decade strain rate.
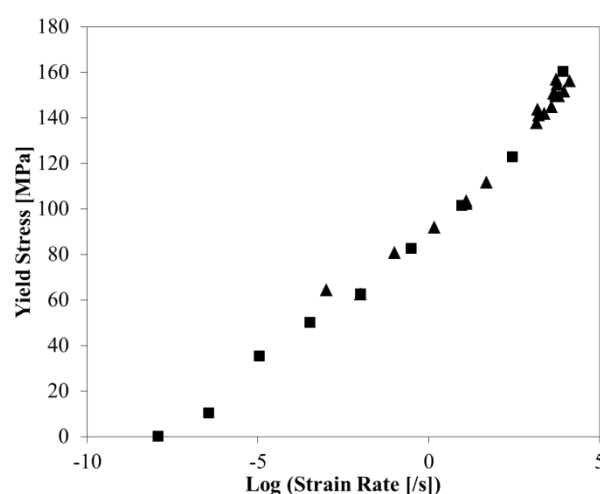
Date	Authors	Page of pages
28 April 2014	CR Siviour, MJ Kendall	38 of 78

Figure 25. PPVC-2: Result from mapping yield stress as a function of temperature (squares) onto strain rate, compared to experimental values of yield stress as a function of strain rate (triangles). The mapping parameter was D = 11 °C/decade strain rate.
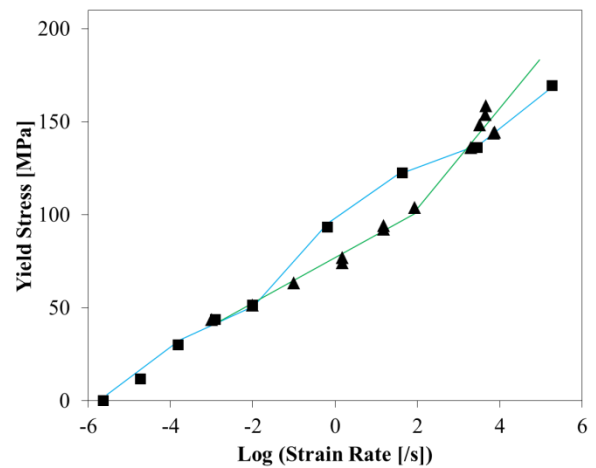
Figure 26. PPVC-4: Result from mapping yield stress as a function of temperature (squares) onto strain rate, compared to experimental values of yield stress as a function of strain rate (triangles). The mapping parameter was D = 8.5 °C/decade strain rate.
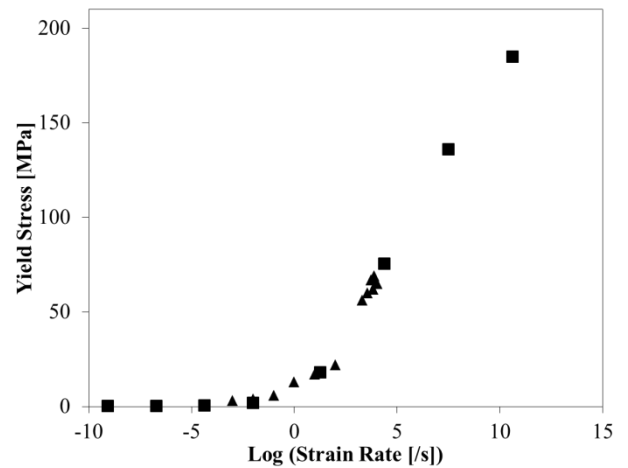
Figure 27. PPVC-6: Result from mapping yield stress as a function of temperature (squares) onto strain rate, compared to experimental values of yield stress as a function of strain rate (triangles). The mapping parameter was D = 7.5 °C/decade strain rate.
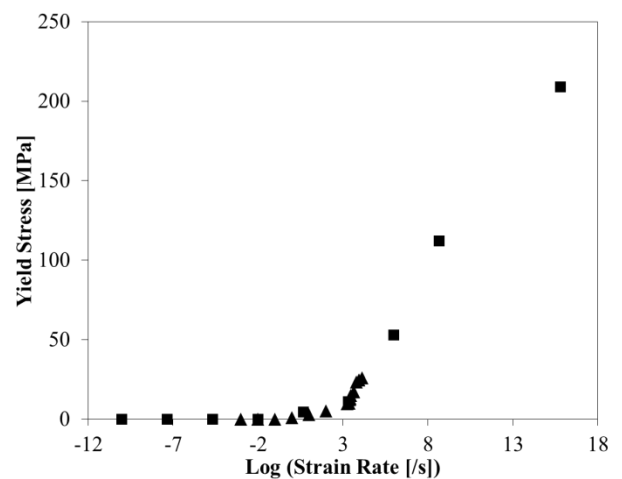
Date	Authors	Page of pages
28 April 2014	CR Siviour, MJ Kendall	39 of 78

Figure 28. PPVC-2 elastic modulus and loss modulus curves at 0.035 s^{-1} (1 Hz – green), 0.35 s^{-1} (10 Hz – blue), and 3.5 s^{-1} (100 Hz – red).
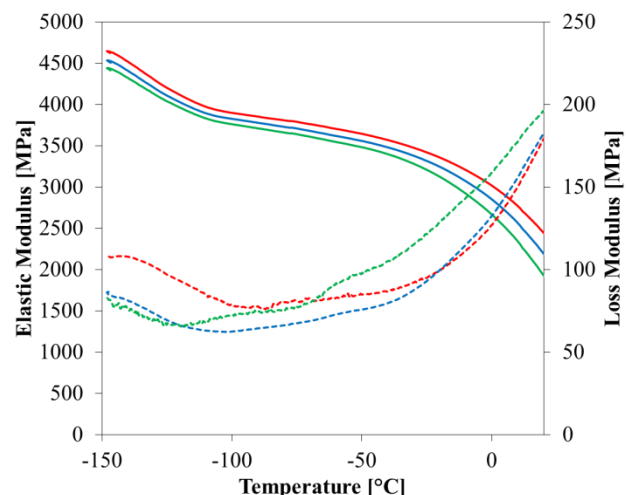
From the higher temperature DMTA data shown earlier in the report, it was found that the α transition shifts at 6 °C/decade strain rate. The result of using this shift in the linear mapping is shown in Figure 29. Using this factor, as opposed to 11 °C/decade strain rate, gives a clear improvement between log(strain rate) = -10 and +3, but not at higher rates. For these higher rate values a second shift factor, this time for the β transition and from the low temperature DMTA data, was obtained: 13.0 °C/decade strain rate. This factor was now applied to the yield stress data to produce the curves in Figure 30.

Hence, for these data it is explicitly recognised that the rate dependencies of the α and β transitions are different, and that their effects on the rate dependency of the yield stress must also be considered separately. This is equivalent to the deconstruct-shift-reconstruct method developed by Mulliken and Boyce [12]to extrapolate high strain rate moduli from DMTA data.

Figure 29. PPVC-2: Result from mapping yield stress as a function of temperature (squares) onto strain rate, compared to experimental values of yield stress as a function of strain rate (triangles). The mapping parameter was D = 6 °C/decade strain rate.
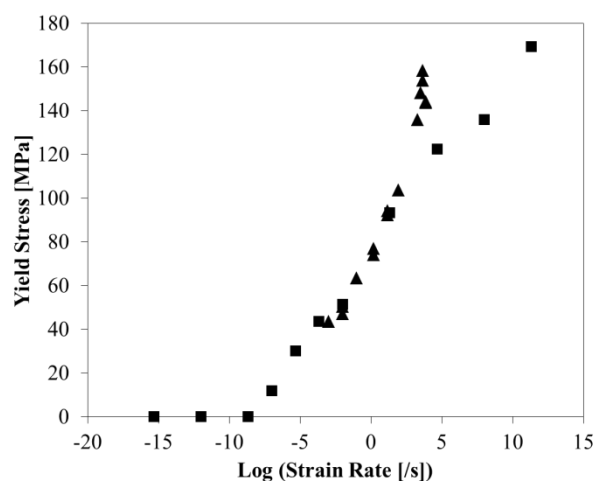
Date	Authors	Page of pages
28 April 2014	CR Siviour, MJ Kendall	40 of 78

Figure 30. PPVC-2: Result from mapping yield stress as a function of temperature (squares and circles) onto strain rate, compared to experimental values of yield stress as a function of strain rate (triangles). The mapping parameters used were $D_\alpha = 6.0$ °C/decade strain rate from 0.001 to 85 s^{-1} (squares) and $D_\beta = 13.0$ °C/decade strain rate for high strain rates 2018 to 7554 s^{-1} (circles).
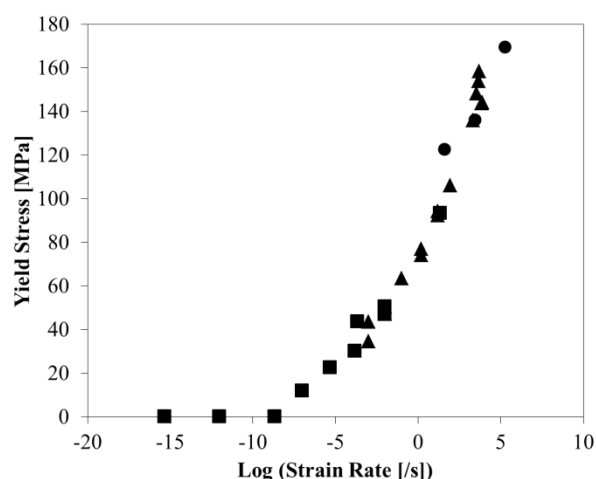
The full set of DMTA data were now used to obtain α and β shift factors, where possible, for all the materials. These were then compared to the shift factors obtained by fitting the yield stresses in Figure 24 – Figure 27, see Table 4, in which there is very good agreement between the two sets of values. In all materials, the β shift factor is larger than the α, potentially the two transitions can merge at very high rates, as is, indeed, observed for PPVC-2. Furthermore, the shift factors for both transitions increase with increasing plasticiser content. A comparison of the DMTA shift factors to those derived from the yield stresses shows again that at high rates, the rate dependence in PVC is dominated by the β transition, whilst that in PVC-2 is affected by both transitions and in PPVC-4 and -6 the α transition dominates.

Table 4. Shift factors obtained from DMTA data compared to those obtained by fitting the yield stress data. Although D_β value for PPVC-6 is listed for comparison, the strain rates and temperatures in the compression experiments did not encompass the β transition for these materials.

Material	D_α DMTA	D_β DMTA	D Yield Stress
PVC	5.35	11.80	13.5
PPVC-2	6.00	13.00	11.0
PPVC-4	7.60	-	8.5
PPVC-6	7.70	16.75	7.5

Date	Authors	Page of pages
28 April 2014	CR Siviour, MJ Kendall	41 of 78

3.3   PVC – Experimentally simulating high rate behaviour in low rate experiments.

3.3.1   Background

The research presented so far outlines the interplay between temperature and strain rate when considering polymer yield stresses. This has only been used descriptively; however the next logical step is to be predictive: to recreate high strain rate behaviour in a low rate experiment. Owing to the requirement for stress equilibrium in high rate experiments, this is of particular interest for low modulus materials (e.g. rubbers and biomaterials) or those with large representative volume elements, requiring large specimens (e.g. composites). Furthermore, this offers the opportunity to perform low strain rate tests with real-time diagnostics for which the acquisition time is too long to be used in high rate experiments. Hence, such a technique will significantly improve our understanding of how microstructure evolution during deformation affects high rate response.

For this reason, a novel experimental method was developed which to experimentally predict and simulate high strain rate stress-strain response expected in a polymer, by performing a low rate experiment at reduced temperatures. The technique was applied to the PPVC-2 material characterised above. A key development is to simulate not only the increase in modulus and yield stress, by reducing the temperature at the start of the experiment, but also the effects of plastic work being converted to heat during the mechanical deformation. In high rate loading this heat does not conduct out of the specimen on the time scale of the deformation, i.e. the deformation is adiabatic. This is done by increasing the temperature of the low rate simulation experiment as it progresses. This technique has the potential not only to avoid several obstacles of high rate testing, such as dynamic equilibrium, but also to allow for microscopic investigation on much smaller length scales through the use of electron and optical microscopy, especially in composite materials in which one component exhibits rate and temperature dependence whilst the other does not. In addition, future development of the technique to increase its fidelity beyond that presented here may provide an opportunity to better understand the mechanisms of high rate deformation, especially the conversion of work to either heat or to structural changes in the material. This will be further explored in section 3.4.

Date	Authors	Page of pages
28 April 2014	CR Siviour, MJ Kendall	42 of 78

3.3.2 Simulating Adiabatic Conditions

In order to simulate a given strain rate, $\dot{\varepsilon}_0$, an initial temperature T' was calculated using the mapping technique, described in the introduction and section 3.2, which relates the dependence of yield stress on temperature at a fixed rate to the dependence on strain rate at a fixed temperature, this is illustrated in Figure 31.

The next stage of the simulation process is to include the effects of adiabatic heating in the specimen, where appropriate. The rate above which the system is expected to behave adiabatically can be calculated from the size of the specimen and the thermal diffusivity of the specimen material using the following equations:

$$\alpha = \frac{k}{\rho C} \tag{11}$$

$$t = \frac{l^2}{4\alpha} \tag{12}$$

$$\dot{\varepsilon} = \frac{1}{t} \tag{13}$$

Here, the thermal diffusivity, α, is first calculated from the conductivity, k, density, ρ, and specific heat capacity, C; alternatively the diffusivity can be found in a number of books. Secondly, a characteristic timescale for thermal diffusion, t, is calculated from a characteristic length-scale l. If l is the length of the specimen, the characteristic timescale thus derived can be converted to a strain rate. Although this is only an approximate calculation, the fact that material response is usually dependent on log(strain rate), means that in practice, when considering rate dependence of material properties, it is only necessary to have an order of magnitude estimate of the transition strain rate from essentially isothermal to essentially adiabatic conditions.
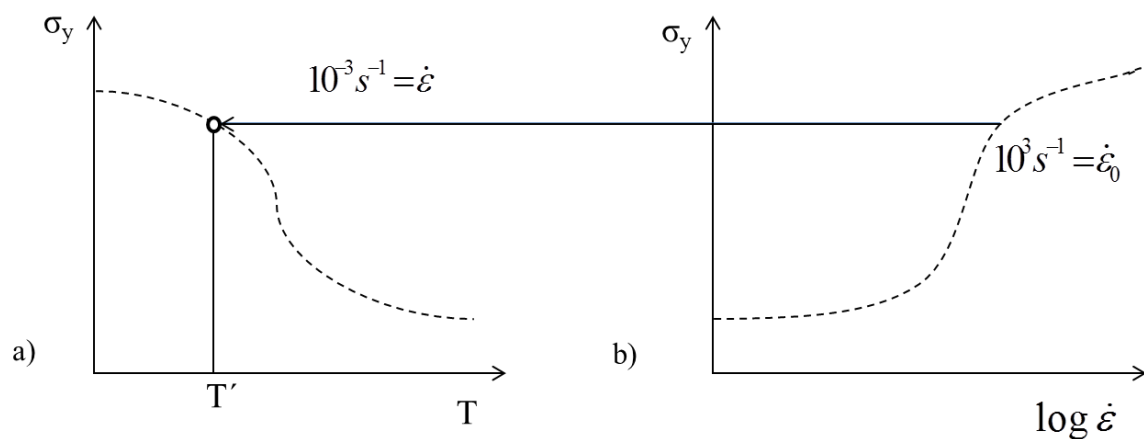
Figure 31. Schematic of yield stress dependence on (a) temperature and (b) strain rate, indicating the process used to find the initial testing temperature to simulate high rate loading.

Date	Authors	Page of pages
28 April 2014	CR Siviour, MJ Kendall	43 of 78

In order to calculate the amount of heating required, the work done must be converted to heat and then to a temperature rise. Specimen heating is assumed to start at the onset of plastic deformation, which in practice can be taken to be the either the start of yielding, or the point of peak stress during yield. This assumption is supported by experimental results, where the temperature rise in polymers during high rate deformation was measured via infrared techniques [24, 26, 27]. Moreover, the experimental data presented in these papers support the assumption that that 100% of the post-yield work put into deforming the specimen is converted to heat, so that the equation

$$\Delta T(\varepsilon) = \frac{\beta}{\rho C} \int_{\varepsilon_y}^{\varepsilon} \sigma d\varepsilon \tag{14}$$

can be used to find the temperature increase as a function of strain, where β, the so-called beta factor, is the fraction of work converted to heat. The area of the stress-strain curve was numerically integrated and the result of this integral is converted to a temperature rise using $\beta = 1$.

The adiabatic temperature rise was simulated in the low rate experiments using the environmental chamber, with the temperature rise being regulated manually at increments of 0.01% strain. The method, including the hypothesised end result, is outlined in Figure 32. The concept is further demonstrated experimentally in Figure 33, by comparing the room temperature stress-strain response of PPVC-2 at 15 s^{-1} to experiments at 10^{-3} s^{-1} and 0 °C with and without the adiabatic simulation. By reducing the initial temperature, the low rate experiment can be made to match the yield stress and initial post-yield softening, but not the large strain response. However, once the post-yield heating is included in the simulation, excellent agreement is observed between the 15 s^{-1} response and the 10^{-3} s^{-1} simulation.
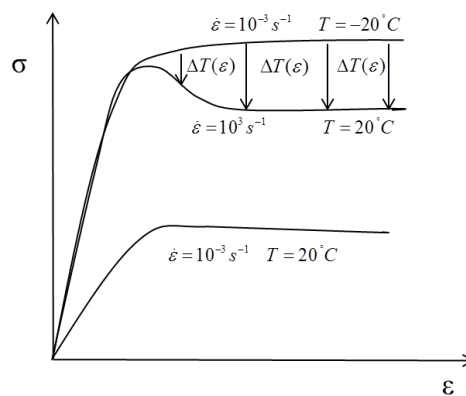
Figure 32. Schematic diagram of the process involved in simulating a high rate experiment (10^{-3} s^{-1}) at a low strain rate with temperature increases during the experiment to simulate the adiabatic conditions under high rate loading.

Date	Authors	Page of pages
28 April 2014	CR Siviour, MJ Kendall	44 of 78
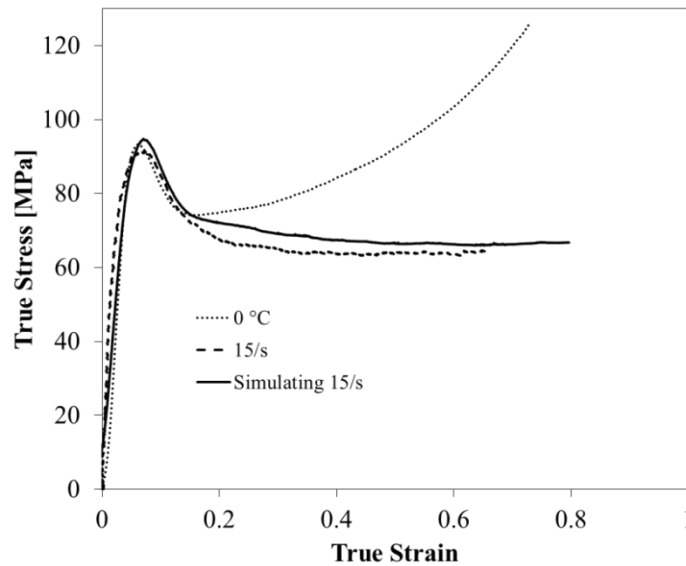
Figure 33. A comparison of PPVC-2 specimen response: at 15 s^{-1} and room temperature; at 10^{-3} s^{-1} and 0 °C, which gives a similar yield to the 15 s^{-1} response; at 10^{-3} s^{-1}, starting from 0 °C but with an appropriate heating profile to simulate the 15 s^{-1} response.

3.3.3   Results and discussion

(a)   (b)
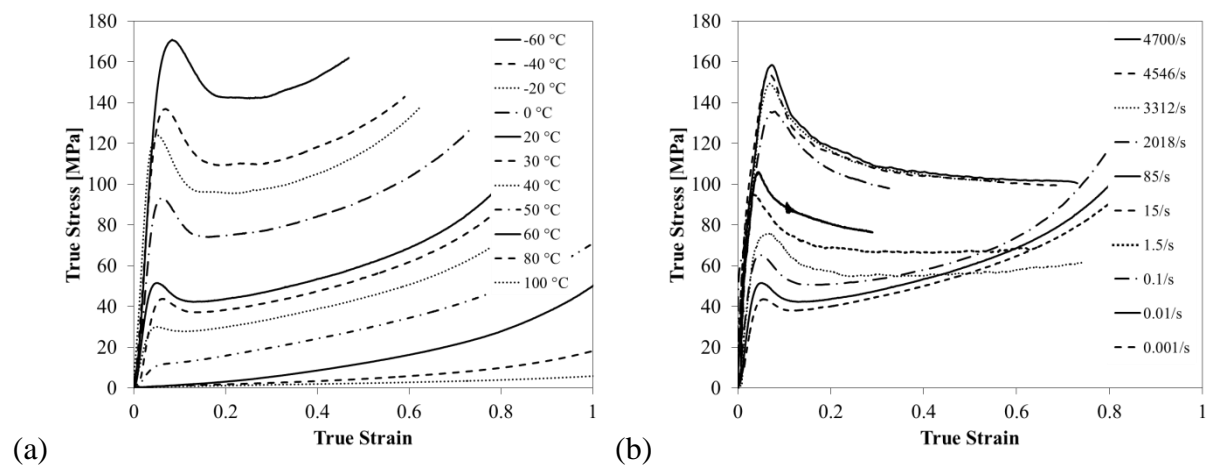
Figure 34. PPVC-2 stress-strain behaviour as a function of (a) temperature 10^{-2} s^{-1} and (b) strain rate at room temperature.

Initial experiments, also reported in section 3.1.4, were performed to evaluate the response of the PVC to loading over a range of strain rates and temperatures (Figure 34).   When comparing the curves at different strain rates, there is a clear transition between those experiments (at rates of 0.1 s^{-1} and below) in which post-yields strain hardening is significant, and those (at rates of 1 s^{-1} and above) in which this hardening is not observed. Using equations

Date	Authors	Page of pages
28 April 2014	CR Siviour, MJ Kendall	45 of 78

(11) – (13) with values of k = 0.1510 W m^{-1} K^{-1}, ρ = 1410 kg m^{-3}, and C = 1 J g^{-1} K^{-1} [51], gives a value of 0.3 s^{-1} as the rate above which deformation would be expected to be approximately adiabatic. The data presented, therefore, are consistent with adiabatic heating playing a role in the reduction of strain hardening at higher rates of strain.

Derived from these stress-strain curves, plots of yield stress as a function of temperature and stain rate (see also section 3.1.4) were used to calculate the initial temperatures required for implementing the simulation technique. As described above, these were chosen to match the yield stress of the rate to be simulated, whilst temperature profiles were obtained by integrating the stress-strain curve.

The experimental data obtained by applying the simulation technique are shown in Figure 35. Here each set of room temperature data is accompanied by the curve obtained by simulating the experiment using a loading at 0.001 s^{-1} with the appropriate temperature profiling. Note that for completeness an additional curve simulating adiabatic loading was obtained at 0.001 s^{-1} even though this does not represent a physically plausible loading condition. The excellent agreement between the SAC stress-strain curves and the curves they were simulating indicates that this is a promising technique for predicting, simulating and understanding high rate behaviour.
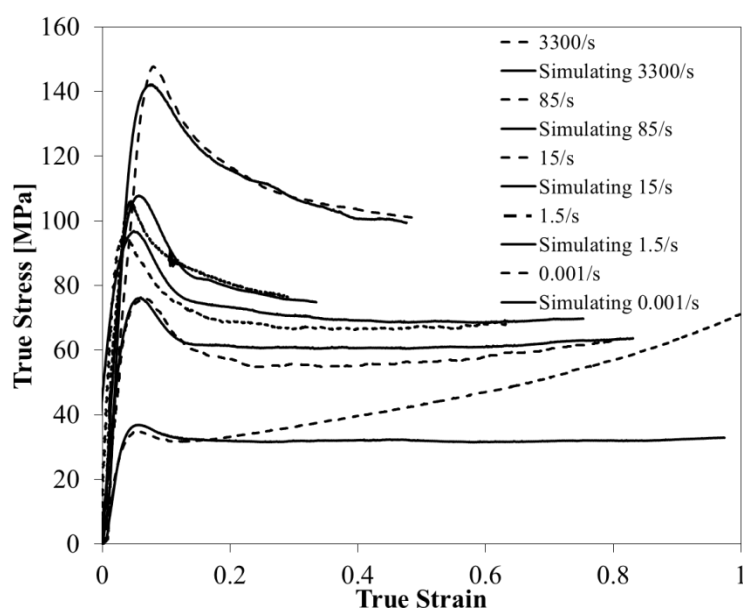
Figure 35. Stress-strain response of PPVC-2 at room temperature and strain rates from 0.001 – 3300 s^{-1} compared to the same strain rates simulated in quasi-static experiments at 0.001 s^{-1} by reducing the initial temperature, and then profiling the temperature to simulate adabatic conditions and 100 % conversion of work to hear. In addition, an experiment simulating adiabatic conditions at 0.001 s^{-1} response is shown to highlight the differences between an isothermal and an adiabatic response.

Date	Authors	Page of pages
28 April 2014	CR Siviour, MJ Kendall	46 of 78

There are a number of possible causes for the discrepancies observed in both the yield and post-yield behaviour. Experimentally, it is difficult to achieve a well-controlled temperature profile in the specimens, due to the thermal inertia in the temperature chamber. Figure 36 shows a typical profile obtained: a smooth 'theoretical' temperature rise is compared to the experimental temperature input actually achieved. In addition, although care was taken to measure the temperature in a number of locations close to the specimen, the specimen may not be in thermal equilibrium with the platens or the surrounding air in the chamber. More positively, the differences may be the result of mechanical behavior of the polymer that has not been accounted for in the simple models used in this project. As the strain rate changes the mechanical processes that govern the observed response are likely to change, especially as the influence of the beta transition changes. In addition, the processes that govern post-yield behavior may not have the same temperature dependence as those that govern yield. Finally, the discrepancies might result from inadequacy in the assumption that all of the work done on the specimen is converted to heat: the beta factor, β, may not be 1. Some of these aspects are explored in the next section.
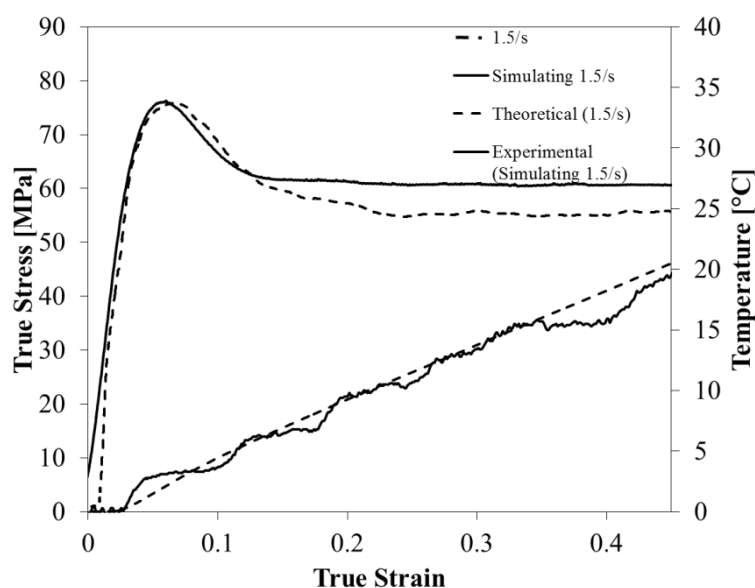
Figure 36. Experimental temperature rise of PPVC-2 during a simulation experiment compared to the target theoretical temperature rise. The corresponding stress-strain behavior of a 1.5 s^{-1} response and the simulated response at 10^{-3} s^{-1} is shown.

Date	Authors	Page of pages
28 April 2014	CR Siviour, MJ Kendall	47 of 78

3.4 Application of experimental simulation to PMMA and PVC

3.4.1 Background

The research presented in this section of the report builds on the simulation method developed in the previous section. Following the success of this approach, further research was performed to investigate PMMA and polycarbonate (PC), chosen due to a number of interesting features in their behaviour. For PMMA, the very low thermal diffusivity means that, for specimens of moderate size, even experiments at 0.1 s^{-1} are essentially adiabatic, and these were simulated using experiments at 0.001 s^{-1}. This gives the opportunity to compare 'real' and 'simulated' data on a single testing apparatus, without the additional complications of high rate testing. A method for measuring temperature rises in these specimens was developed, section 3.6, and data obtained were used to refine the simulation. For PC, the effect of different β factors was investigated, motivated by observations in the literature that the rate dependence of strain hardening in this material is less than might be expected from the measured temperature rises. Interesting results were obtained on both materials, and these are discussed in the context of current literature. As well as the results themselves, this section shows how the simulation technique can be used to better elucidate and understand the interplay between temperature and strain rate in governing the mechanical response of polymers under large strain deformation.

3.4.2 PMMA – background and preliminary results

PMMA is used in many engineering applications and a large amount of literature has been focused on its strain rate and temperature dependence [2, 10, 12, 16, 52-54]. Similar to other amorphous polymers, PMMA has shown a clear interplay between rate and temperature dependence, with increases in yield strength and elastic modulus with increasing strain rate and decreasing temperature. PMMA presents particularly interesting material behavior as the effect of the β transition is observed at room temperature at lower strain rates (~ 10^{-2} s^{-1}) than in the PPVC specimens tested in the previous chapter. Furthermore, the low thermal conductivity means that specimen heating also occurs at lower strain rates than for PVC.

Before performing the adiabatic simulation experiments, a thorough characterization of the material was carried out in compression and using a DMTA. Specimens were machined from a 25.4 mm diameter PMMA rod; samples for quasi-static experiments were 8 mm diameter and 8 mm long, whilst those for high rate experiments were 8 mm diameter and 3.5 mm long.

DMTA data are shown in Figure 37. An important feature of this material is that the β

Date	Authors	Page of pages
28 April 2014	CR Siviour, MJ Kendall	48 of 78

Figure 37. PMMA storage modulus and loss modulus as a function of temperature at 1 Hz (~0.035 s^{-1}), 10 Hz (~0.35 s^{-1}), and 100 Hz (~3.5 s^{-1}).
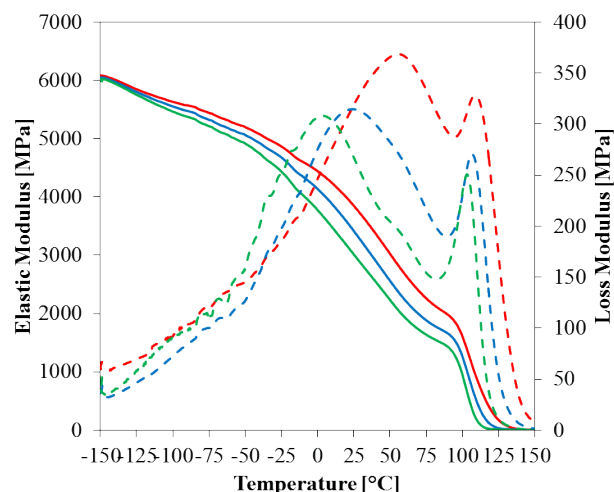
transition occurs around room temperature, and that the β and α transitions merge at quite modest frequencies. The shift factors for the two transitions are 5 °C/decade strain rate for α and 25 °C/decade strain rate for β; hence, they continue to merge as the strain rate increases. The α shift factor is approximately 5 °C/decade strain rate lower than that found in literature (5 vs. 10 °C/decade strain rate), whilst the β shift factor is equivalent to the literature [12]. The shift of the β transition to higher temperatures as the strain rate increases leads to a transition from ductile to brittle behaviour with increasing strain rate.

Stress-strain and yield stress data as functions of temperature and strain rate are given in Figure 38 and Figure 39. In the low strain rate experiments, all specimens deformed in a ductile manner above -60 °C, which saw brittle failure at ~35% true strain, and -87 °C which saw brittle failure just after the maximum stress during yield at ~10% true strain. As the rate was increased, at room temperature, specimens tested below 0.1 s^{-1} did not fail, those tested at 1, 10 and 80 s^{-1} failed at c.a. 40% strain and those tested at about 2500 s^{-1} failed at about 10%.

(a)

(b)
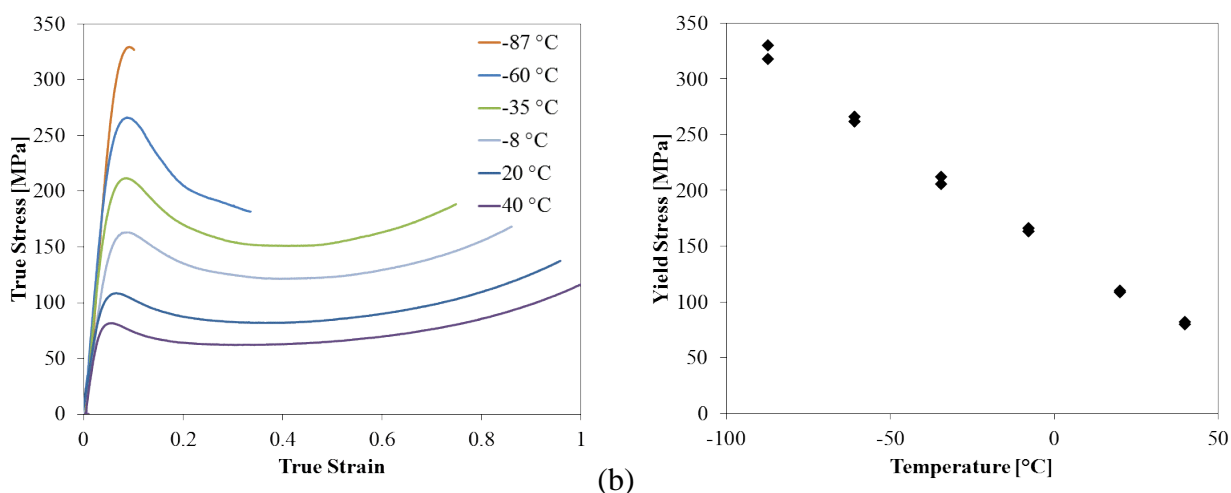
Figure 38. PMMA (a) Stress-strain response at a strain rate of 10^{-2} s^{-1} and temperatures from -87 – 40 °C. (b) Yield stress at a strain rate of 10^{-2} s^{-1} as a function of temperature.

Date	Authors	Page of pages
28 April 2014	CR Siviour, MJ Kendall	49 of 78
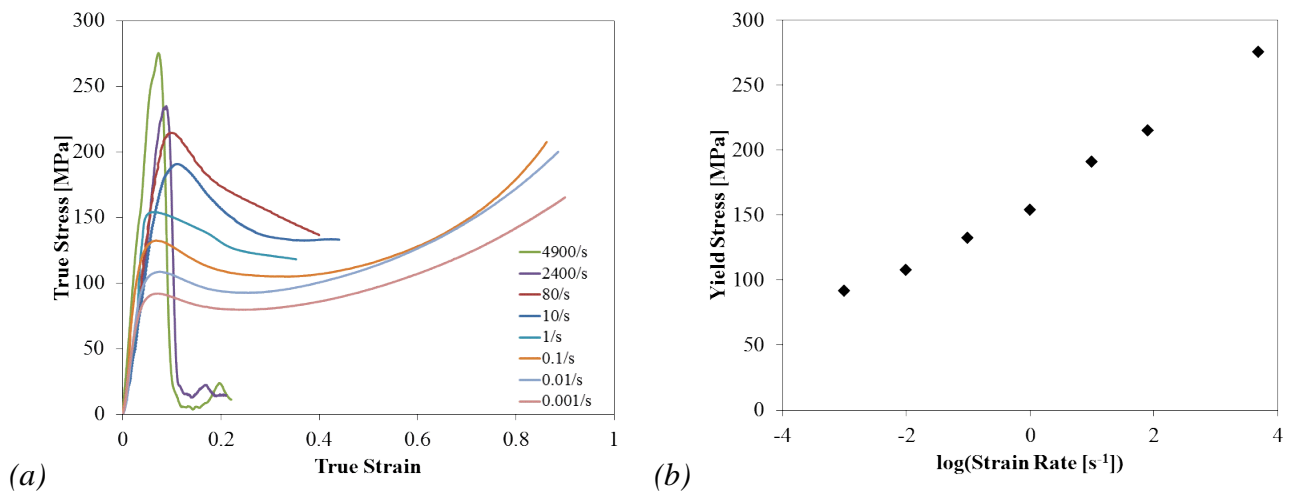
Figure 39. PMMA (a) Stress-strain response at room temperature and strain rates from 0.0005 s^{-1} – 2500 s^{-1}.(b) Yield stress at room temperature as a function of strain rate.

3.4.3   PMMA – Simulating Adiabatic Conditions

The thermal diffusivity of PMMA is 0.11 mm^2 s^{-1}, giving a characteristic time of 150 s for heat to diffuse out of the specimen. Experiments were therefore performed at a rate of 0.001 s^{-1} and an initial temperature of -7.25 °C, to produce the same yield stress as a room temperature experiment at 0.1 s^{-1}. The temperature was increased during the experiment assuming a *β* factor of 1 and fully adiabatic conditions. The stress-strain curve obtained, Figure 40 agreed closely with the curve it was simulating, the differences between the curves being similar to the variability one would normally expect when testing multiple specimens.

Following this very encouraging result, a number of methods were investigated to measure the real temperature rise in a specimen tested at 0.1 s^{-1}. Because of the semi-brittle nature of PMMA, it was not possible to do this using thermocouples inserted into holes in the specimen. Instead, a new thermocouple system was designed which can be sandwiched between two half-length specimens, section 3.6, and was shown both not to interfere with the measured mechanical response of the specimen and to measure the temperature up to true strains of at least 1. The temperature rise measured was less than that assumed in the initial simulation experiment, which may be attributed to the *β* factor being less than 1, or the conditions not being fully adiabatic.

Date	Authors	Page of pages
28 April 2014	CR Siviour, MJ Kendall	50 of 78
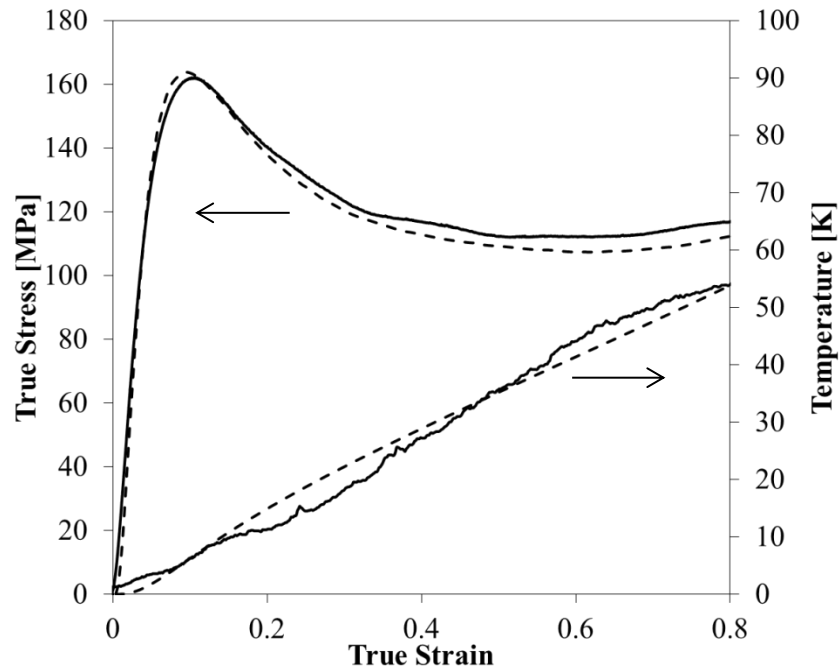
Figure 40. PMMA true stress-true strain behaviour in uniaxial compression at 0.1 s^{-1} (at 20 °C): experiment (dashed line) with its theoretical temperature rise, and experimental simulation (solid line) with the temperature input.

Further investigations were also performed using a thermal camera to look for temperature gradients in the specimen, none were observed, and replacing the steel anvils with more insulating, plastic, ones, which made no difference to the measured stress-strain response. Although these experiments are not wholly conclusive, they indicate that the experimental conditions are adiabatic, and therefore that either the *β* factor is less than 1 or the heat capacity changes when the specimen yields. The simulation experiment was therefore repeated using the measured temperature rise, the result of which shown in Figure 41. It is clear that using this temperature rise gives less strain softening and more strain hardening in the simulation experiment compared to the 'real' data and the other simulation curve. This indicates that, although not all the work done on the specimens at the higher strain rate is being converted to heat, it is all contributing to increased molecular mobility within the material, which requires higher temperature rises to simulate using heat alone. These observations will be discussed further below[2].

---

[2] It is noted that in this second simulation experiment more work is done on the specimen, indicating that a slightly higher temperature rise is justified, however, the difference in work is only approximately 2.5 %.

Date	Authors	Page of pages
28 April 2014	CR Siviour, MJ Kendall	51 of 78
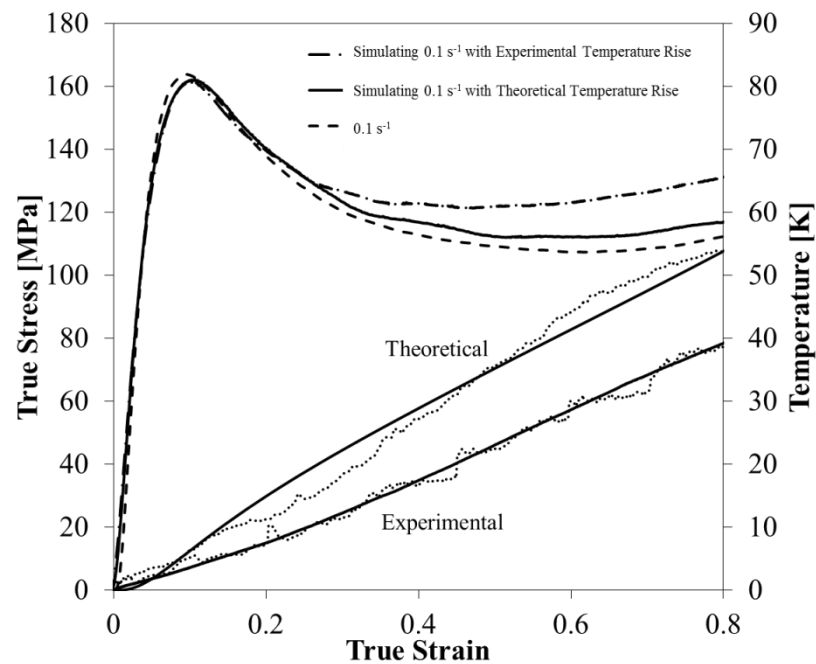
Figure 41. PMMA true stress-true strain behaviour in uniaxial compression at 0.1 s^{-1}, compared to simulation data produced using the experimental temperature rise and the theoretical temperature rise. For the temperature rises, solid lines show the target values whilst dotted lines show the temperatures achieved in the experiment.

3.4.4 Polycarbonate – background and preliminary results

The mechanical properties of polycarbonate (PC), like PMMA, have been extensively studied in the literature, [3, 10-12], including a number of studies of its temperature rise at high rates of deformation [26, 27, 55, 56]. Regev and Rittel [25, 26] used thermocouples to measure the temperature rise in polycarbonate specimens undergoing high rate deformation and later confirmed the accuracy of this method via infrared techniques, and found that conversion was approximately 100%, Garg et al. [27] obtained the same result. However, Li and Lambros, using high speed infrared detector array at rates around 10^3 s^{-1}, found that the amount of plastic work converted to heat for PC ranged from 50% to 100% depending upon the applied strain [56], and data from Mulliken [57] indicate a value of about 80%.

Similar to other amorphous polymers, PC shows a clear interplay between rate and temperature dependence while exhibiting increases in yield strength and elastic modulus with increasing strain rate and decreasing temperature. In previous work, Mulliken [12, 57] applied a model for rate dependent mechanical response of polymers to a number of different materials. The model [57] included a term to simulate adiabatic conditions, which could be switched on and off as required. Using this term where appropriate the model was able to

Date	Authors	Page of pages
28 April 2014	CR Siviour, MJ Kendall	52 of 78

capture strain softening, and the difference between adiabatic and isothermal conditions, in a number of polymers, but not polycarbonate (PC). A number of other researchers [3, 10, 14, 26, 27, 55, 56, 58] have studied the rate dependence of PC, and the available data indicate that, unlike the PMMA and plasticised PVC discussed above, the amount of strain softening after yield does not increase with strain rate, nor does the amount of strain hardening decrease: instead, there is a decrease in strain softening, and an increase in strain hardening. These observations are unexpected: although available measurements of temperature rises in PC under high rate deformation show somewhat differing results the data at rates of around 2000 s^{-1} point towards 80% conversion of work to heat in high rate loading.

These seemingly contradictory observations make PC an ideal candidate for further investigation using the simulation method.

Experiments were performed on a commercial, extruded PC rod, the loading axis of the specimens is aligned with that of the rod, and specimens were right cylinders 2.5 mm long and 5 mm in diameter. The thermal diffusivity is 0.11 mm^2 s^{-1}, so we expect the characteristic timescale for heat diffusion out of the specimen to be about 10 s. Quasi-static and high rate room temperature data were obtained, Figure 42, supplemented by enough temperature dependent data to identify the initial temperature required to simulate the high rate loading, Figure 43. The effect of the β transition, which in polycarbonate is very distinct from the α, with up to a 100 K temperature spacing between the two transitions [3, 57], is clearly observed in the rate dependence.
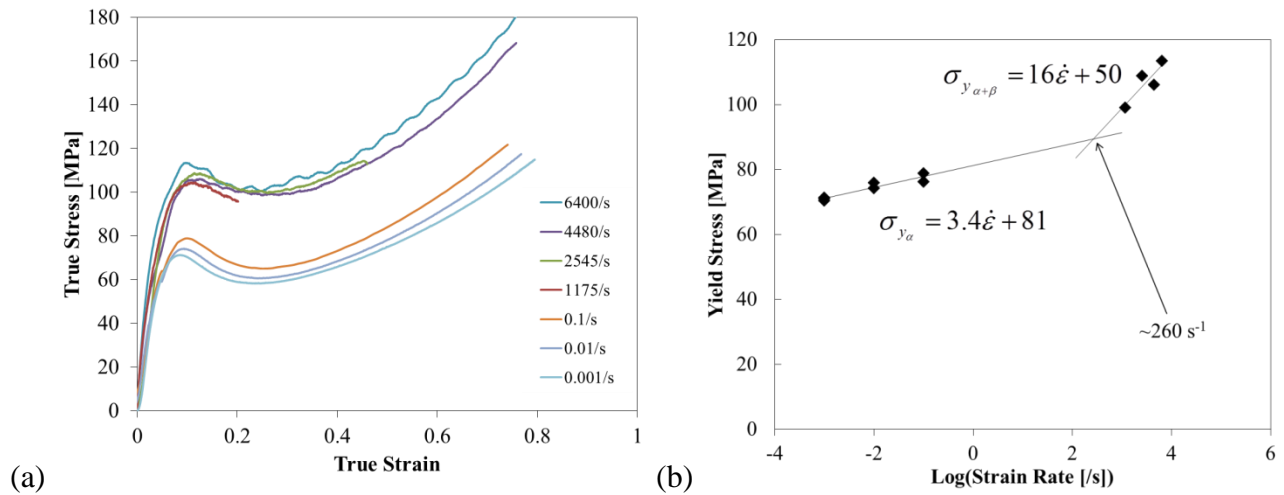
Figure 42. PC (a) True stress-true strain response at strain rates from 10^{-3} s^{-1} – 6400 s^{-1}; (b) yield stress as a function of (log) strain rate (10^{-3} s^{-1} – 6400 s^{-1}).

Date	Authors	Page of pages
28 April 2014	CR Siviour, MJ Kendall	53 of 78
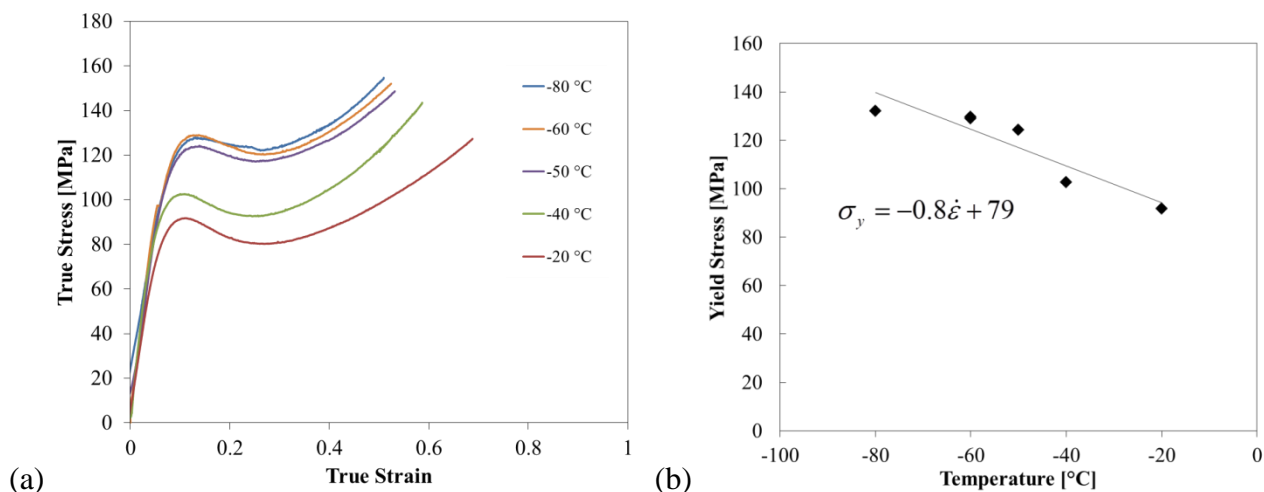
Figure 43. PC (a) stress-strain response at temperatures from -80 – -20 °C and a rate of 10^{-2} s^{-1}; (b) yield stress as a function of temperature (-80 – -20 °C).

3.4.5 Polycarbonate - Simulating Adiabatic Conditions

A number of experiments, all at 0.001 s^{-1} with an initial temperature of -46 °C, were performed to simulate the high rate response at 2550 s^{-1}; the results of these experiments are shown in Figure 44. Initially, a β factor of 1 (and fully adiabatic loading) was assumed, but the simulation experiment showed completely different post-yield behaviour to the 'real' high rate data. The assumed β factor was then decreased a number of times, until eventually, at β = 0.05, the simulated stress-strain curve matched the high rate data. It can be seen from the figure that this results from a very small temperature rise. This implies that, despite the fact that in reality nearly all the applied work is converted to temperature rise in high rate loading of PC, the material behaves as if the temperature rise is very small, and hence further work is required to fully understand the mechanisms that govern post-yield response and PC's lack of sensitivity to thermal changes due to the heat created during high strain rate loading.

3.4.6 Discussion

The adiabatic simulation technique has now been applied to three polymers: PVC, PMMA and PC with very different results. In all three cases, experiments at 0.001 s^{-1} were used to simulate higher rate loading by increasing the starting temperature of the experiment and the increasing the temperature during the experiment to simulate the adiabatic conditions in the materials. Although the simulated rates were different: 10^{-3} to 3300 s^{-1} for 20 wt % plasticised PVC, 2550 s^{-1} for PC and 0.1 s^{-1} for PMMA, in all three cases the beta transition plays a role

Date	Authors	Page of pages
28 April 2014	CR Siviour, MJ Kendall	54 of 78

in the mechanical response. In fact, for plasticised PVC, the simulations encompass both higher rates at which the beta transition does affect the response, and lower rates in which it does not.

However, it is clear that there is a difference in the outcomes of the simulation experiments, which may indicate underlying differences in their post-yield mechanics:

- In PVC, a β factor of 1 was assumed, which is supported by measurements at high rates. This assumption led to good simulation of high rate behaviour;
- In PMMA, a β factor of 1 led to good simulation, but was in fact too high; using the real temperature rise in the specimen led to a simulated stress that was above the real value;
- In PC, a β factor of 1, although consistent with data from the literature, led to a simulated stress below the real value. The β factor had to be reduced to 0.05 for an accurate simulation; this is far below any measured values reported in the literature.
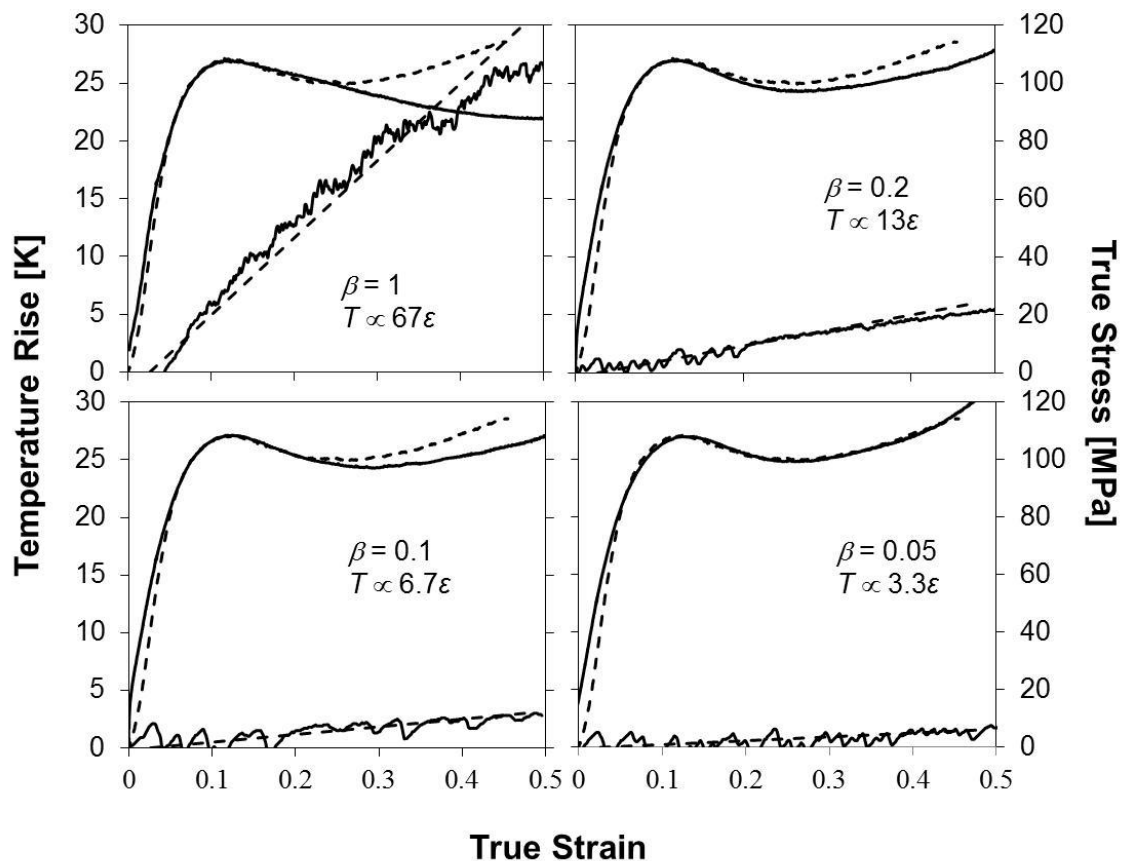
Figure 44. Results from simulating the polycarbonate stress-strain relationship at 2550 s^{-1} in experiments at 0.001 s^{-1} using four different β factors. High rate stress-strain curves are solid, simulation curves dotted. For the temperature data the intended temperature profile is dotted and the real profile is solid. The starting temperature was -7.25 °C in all cases.

Date	Authors	Page of pages
28 April 2014	CR Siviour, MJ Kendall	55 of 78

From the PMMA temperature rise data, the energies of deformation can be calculated at a strain rate of 0.1 s^{-1}. The work of deformation is calculated from the stress-strain curve, whilst the heat of deformation comes from the temperature rise in the specimen. The remaining energy is called the internal, or stored, energy (33, 38). Figure 45 shows these three values as functions of strain. Approximately 75% of the work is converted to heat; the stored energy increases rapidly until a strain of about 0.3 and then more slowly for the remainder of the experiment; this is consistent with Rudnev's data on PC [59]. It is well known that in quasi-static deformation of amorphous polymers there is a structural evolution towards a less compact higher energy structure with lower flow stress, which causes strain softening in the observed response [60]. This evolution is endothermic, and hence in the experiment at 0.1 s^{-1}, the heat of deformation is less than the work done on the specimen. When simulating the behaviour at 0.001 s^{-1} *and reduced temperature* all of this energy must be replaced by thermal energy in order to replicate the stress-strain curve.

These observations illustrate that a majority of the strain softening seen in the true stress-strain behaviour is indeed caused by the heat of deformation, but the remainder of the strain softening is caused by a material characteristic seen only in the higher rate of deformation (0.1 s^{-1}), and which is not accommodated by the rate of deformation in the simulation tests (0.001 s^{-1}).

As an aside, the results from these experiments have implications for quasi-static data in the literature, and for the use of these data to simulate deformation of structures: even for small specimen sizes and low strain rates, heating can play a major role in the observed mechanical response of the specimen to deformation.
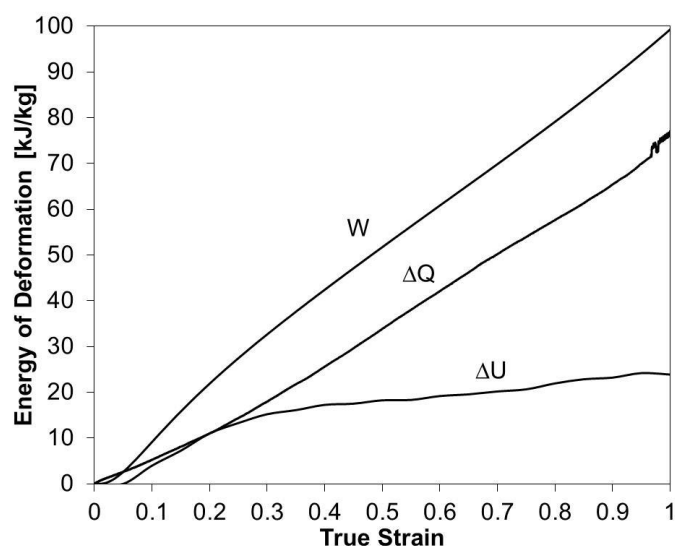
Figure 45. Energies of deformation in PMMA: W = mechanical work of deformation; ΔQ = heat of deformation; ΔU = internal or 'stored energy'.

Date	Authors	Page of pages
28 April 2014	CR Siviour, MJ Kendall	56 of 78

For PC, the observations are almost opposite: although the temperature increases significantly in high rate loading, according to the simulation technique only a small rise is required to reproduce the post-yield behaviour observed. It appears logical to suggest that this is associated with the beta transition in this material, although it must be noted that the vary basis of the simulation method is that the high rate and low temperature data are both affected by this transition, or at least that the yield stresses are. Hence the data indicate that there is some aspect of the strain softening / post yield behaviour, which may indeed be associated with the beta motions, for which the interplay between rate and temperature dependence is different from that of the yield stress, and which must be captured in order to produce a successful high rate constitutive model.

3.5 Application to PBS in tension and compression

3.5.1 Background

Having established the experimental simulation technique for replicating the high rate behaviour of polymers, and applied it to three different polymeric materials, the research in this section aimed to apply the same technique to a composite material consisting of a rate and temperature dependent binder with a rate and temperature *in*dependent filler. In this case, a polymer bonded sugar (PXS) was used. This was chosen because of its relatively simple behaviour (compared to fibre reinforced composites) and the widespread interest in these materials because of their use as mechanical simulants for polymer bonded explosives, which means that there is a good body of literature on the materials.

Although this chapter is mainly concerned with the use of PBSs as a model material for the simulation technique, a brief overview of the literature is given here.

Polymer bonded explosives (PBXs) are seen in a wide range of applications, from the central explosive charge in standard armaments to rocket propellants. In armaments, PBXs typically contain 2-10% (by mass) of polymer, or up to 40% for rocket propellants – the polymer acts as a load mitigator to improve safety in in storage and handling and is typically a rubbery material (e.g. hydroxyl-terminated polybutadiene, HTPB and other polyurethane-based compositions). The second component of the PBXs typically consists of an explosive in the form of small crystals, such as cyclotetramethylene-tetranitramine (HMX), pentaerythritol-tetranitrate (PETN), cyclotrimethylenetrinitramine (RDX), or triamino-trinitrobenzene (TATB) [61, 62]. For PBX simulants, such as the material used in this study, the explosive substitute is typically a sugar crystal (mainly due to the availability of comparable particle sizes and similarities in the mechanical behaviour).

Bowden and Yoffe [63, 64] were among the first to study ignition mechanisms in explosives and concluded that explosive ignition reactions begin at localized 'hot spots.' Further investigations have offered insight into impact ignition [65-68] and its two-step process: an initiation step and a propagation step [65, 69]. The use of a binder suppresses both of these steps, and hence reduces the sensitivity of the explosive considerably.

Swallowe and Field [70] studied the mechanical properties and sensitivity of polymer bonded explosives and found a wide range of differences depending on the characteristics of the polymer binder. Surface, thermal, and mechanical properties must all be considered when examining the choices for a binder material.

Palmer *et al.* [61] examined a wide range of PBXs with different compositions in tension at quasi-static strain rates, and were the first to use the Brazilian test to study tensile behaviour. The main advantage of the Brazilian test being the use of small specimens and the

Date	Authors	Page of pages
28 April 2014	CR Siviour, MJ Kendall	58 of 78

ease of both manufacturing and mounting, compared to more traditional tensile tests using dog-bone specimens, and the configuration has been used in both quasi-static [71] and dynamic [46] testing.

Over the past fifteen years, a wide range authors have presented data from investigations of polymer bonded explosives and their simulants under high rates of deformation [8, 9, 72-80]. These investigations found a clear rate, and temperature dependence, which can be attributed to the binder: although the binder only constitutes a small proportion of the mass it has a significant effect on the mechanical properties, especially up to loading densities of c.a. 90%, above which crystal-crystal interactions become more prevalent. Williamson *et al.* [9] and Thompson et al. [8], both present successful results from time-temperature superposition of PBX yield stresses.

3.5.2 Materials and experimental details

The polymer bonded explosive simulant used in this chapter (DM076) consisted of 83% caster sugar, of both coarse (400-600 μm) and fine (10-110 μm) diameters, in a HTPB binder. Expeiments were performed on both the PBS and the binder. Both materials were manufactured at the High Explosives Research and Development (HERD) facility of the Energetic Materials Branch of Air Force Research Laboratory, in Eglin, FL, USA. Tests specimens were all right cylinders 10 mm diameter × 4 mm thickness.

High rate experiments were performed using the split Hopkinson bar arrangement with Titanium alloy bars: for the HTPB specimens, additional high sensitivity stress gauges, described in the next section, were used.

Brazilian tests were performed using platens with a radius of 6 mm. For the high rate experiments these were mounted on the Hopkinson bars. In both low and high rate experiments, force time data were obtained, which were converted to stress-time using equation (10). Strain data were obtained for a subset of the experiments using digital image correlation (DIC). Commercial DIC software was used to produce displacement maps from images taken using a Nikon DSLR camera in the low rate experiments, and a Photron SA5 high speed camera at high rates. The displacements across the centre of the specimen, perpendicular to the loading direction, were then used to calculate strain. The contact half radius (b) in equation (10) was also measured from these photographs.

3.5.3 Stress gauges

The HTPB supplied was found to have a very low strength at room temperature. This led to two difficulties in the high strain rate experiments: signal to noise ratio on the transmitted stress pulse from which the stress is calculated, and the difficulty in establishing the force on

Date	Authors	Page of pages
28 April 2014	CR Siviour, MJ Kendall	59 of 78

the front face of the specimen in order to confirm stress equilibrium. The latter problem arises from the need to find the small difference between two very large forces.

In order to overcome these difficulties, piezoelectric gauges were used to measure the stresses directly at the specimen-bar interface. The gauges were mounted, using a conducting adhesive, between two thin metal disks which acted as electrodes: thin wires were welded to these electrodes in order to connect to a charge integrator. The whole package was attached to the bars using an insulating glue, see Figure 46. Piezoelectric materials produce a charge difference proportional to the force applied to them, and the charge integrator converts this to a voltage. The material used here was lead zirconium titanate (PZT), which is approximately 100 times more sensitive than the quartz materials typically used in the literature. In this case, the sensitivity is given by the manufacturer as 400×10^{-12} C/N, compared to 2×10^{-12} C/N for a typical quartz gauge. When mounted on the Hopkinson bar, attached to the charge integrator and calibrated, this resulted in a gauge factor of 0.0079 and 0.0171 V/N for the input and output gauges respectively.

Figure 47 compares force-time data from the standard Hopkinson bar gauge and the PZT gauges, showing the great improvement that results from the use of these gauges.
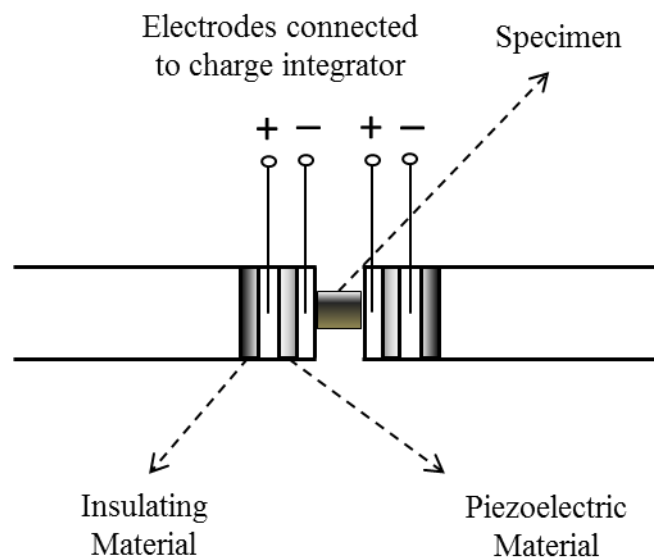
Figure 46. Schematic diagram of the piezoelectric strain gauge system

Date	Authors	Page of pages
28 April 2014	CR Siviour, MJ Kendall	60 of 78
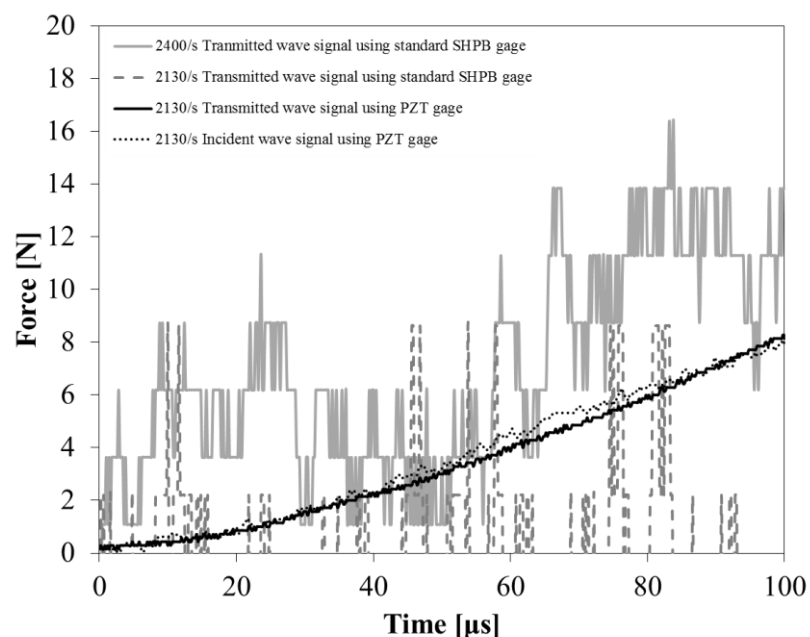
Figure 47. Comparison of force time data on HTPB rubber: a *magnesium alloy* bar at 2400 s^{-1}; a titanium alloy bar at 2130 s^{-1} and the two PZT gauges mounted on the titanium alloy bar at 2130 s^{-1}. Note that the titanium alloy curves are from the same experiment, and that magnesium alloy Hopkinson bars are typically 2× more sensitive than titanium.

3.5.4 Results and discussion

The HTPB and PBS DMA test results are summarized in *Figure 48*. The α transition of the HTPB is very low (ca. -85 °C), with the beginning of a very broad β transition at approximately -100 °C, in the 100 Hz curve. The data allow shift factors to be found: 6 °C/decade for the α transition and a 20 °C/decade for the β transition. The α transition of this HTPB is approximately 25 °C lower than that found in literature [80]. However, it should be recognised that the properties of HTPB are highly dependent on the manufacturing process.

The PBS also presents rubbery behaviour with an α transition at approximately 70 °C, with again the possibility of a β transition at lower temperatures. Because the filler has a modulus many orders of magnitude higher than the binder, all the applied deformation is taken up in the binder, meaning that for a given magnitude and frequency of oscillation, the effective strain rate in the binder is higher, and the α transition temperature increases, compared to the pure HTPB. The general behaviour of the PBS is consistent with observations in the literature, that the α transition is at a higher temperature and broader than that of the binder. However, the low α transition temperature of the binder also carries through into the PBS, for example the α transition of the PBS used by Siviour *et al.* is -60 °C higher [9, 79, 80].

Date	Authors	Page of pages
28 April 2014	CR Siviour, MJ Kendall	61 of 78

Uniaxial compression testing results are summarized in Figure 49 and Figure 50. During quasi-static temperature dependence testing, all HTPB specimens deformed in a rubbery manner at temperatures above -90 °C, with a glassy region beginning sharply below this temperature. The behaviour at -100 °C presents interesting characteristics: because these tests are centred around the glass transition temperature, slight changes in temperature bring about large changes in modulus, yield stress, and post-yield behaviour; hence, even when testing at nominally the same temperature (-100 °C) a wide range of yield stresses is observed from roughly 10 MPa to just below 40 MPa.

(a)   (b)
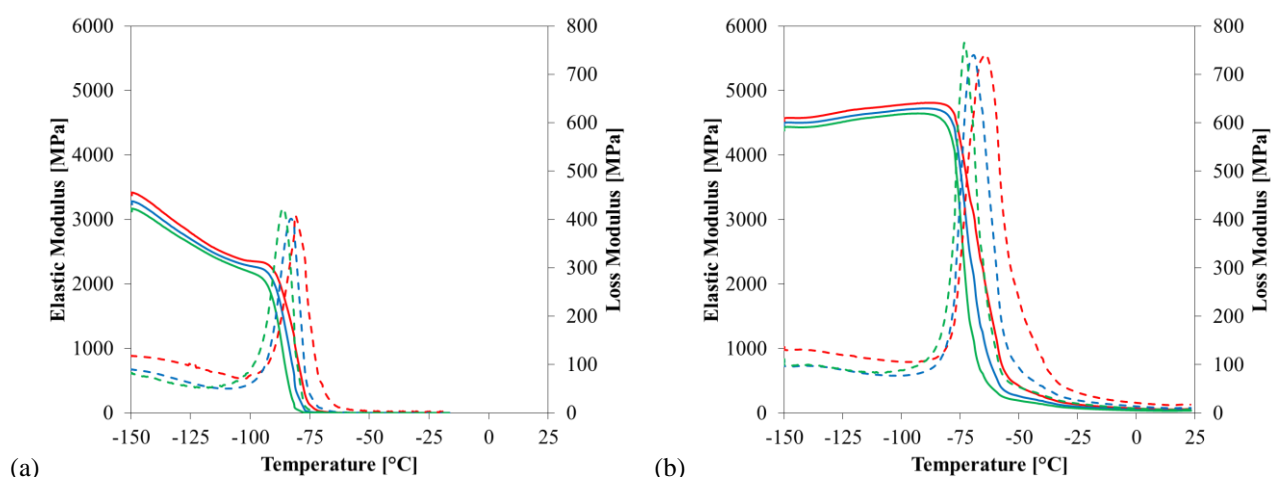
Figure 48. (a) HTPB and (b) PBS: elastic modulus (solid lines) and loss modulus (dashed lines) as a function of temperature at 1 Hz (0.032 s^{-1} – light grey), 10 Hz (0.32 s^{-1} – dark grey), and 100 Hz (3.2 s^{-1} – black).

(a)   (b)
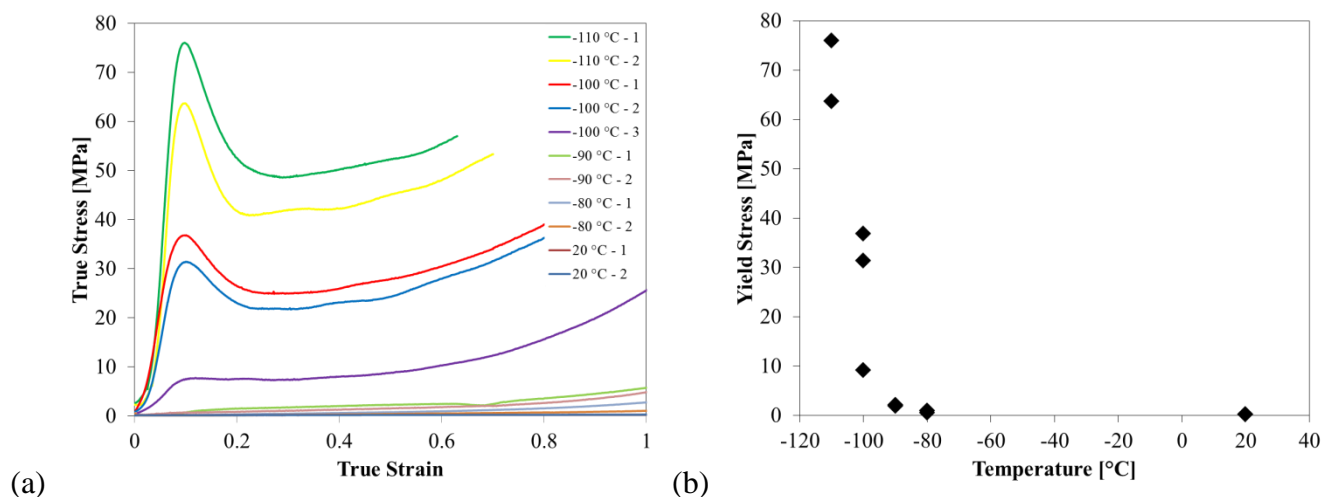
Figure 49. HTPB (a) true stress-true strain and (b) yield stress behaviour as a function of temperature (-110 – 20 °C) at a rate of 10^{-2} s^{-1}. Note: for (b) trues stress data at 0.1 true strain is reported above -80 °C.

Date	Authors	Page of pages
28 April 2014	CR Siviour, MJ Kendall	62 of 78

Figure 50. Representative true stress-true strain behaviour of HTPB as a function of strain rate (10^{-3} – 3450 s^{-1}) at an ambient temperature of 20 °C.
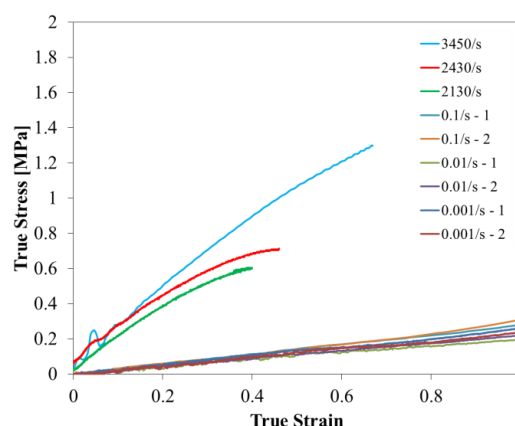
The HTPB true stress-true strain behaviour demonstrates increasingly glassy polymer characteristics when moving towards lower testing temperatures: a dramatic post-yield softening is visible at -110 °C where yield is measured at 77 MPa, and subsequently a softening of magnitude ~27 MPa is observed. In the PBS (Figure 51), a maximum strain softening of 10 MPa is observed in true stress-true strain behaviour at -80 °C.

The α transition in HTPB (Figure 49) is between -90 °C and -100 °C (at 10^{-2} s^{-1}) which is consistent with the DMTA at 0.032 s^{-1}. Comparison between PBS data sets is more interesting: the quasi-static compression data at room temperature appear to show glassy behaviour (Figure 52), although there is no apparent contribution of the glass transition at these rates and temperatures (20 °C) in the DMTA data. The observed behaviour is likely due to gradual debonding of the crystals from the binder as observed by Siviour *et al.* [80]. Comparing rate dependent data from HTPB (Figure 50) and PBS (Figure 52); in the PBS, this pseudo-glassy behaviour is seen in all true stress-true strain rate dependent behaviour, where in HTPB, the response continues to be rubbery even at high strain rates (up to 3450 s^{-1}).

(a)   (b)
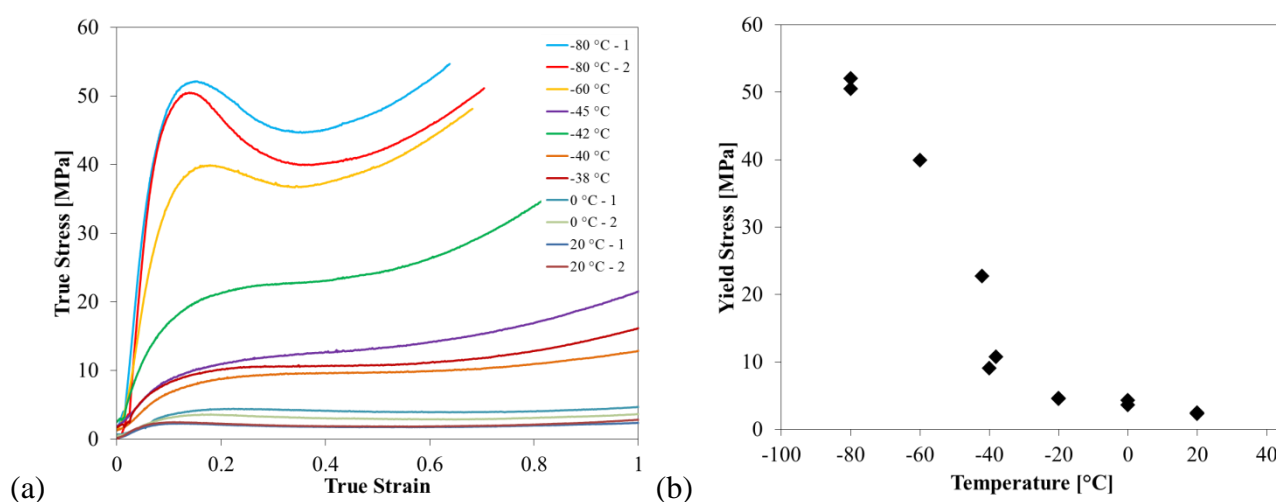
Figure 51. PBS (a) true stress-true strain behaviour and (b) yield stress behaviour as a function of temperature (-80 – +20 °C) at a rate of 10^{-2} s^{-1}.

Date	Authors	Page of pages
28 April 2014	CR Siviour, MJ Kendall	63 of 78
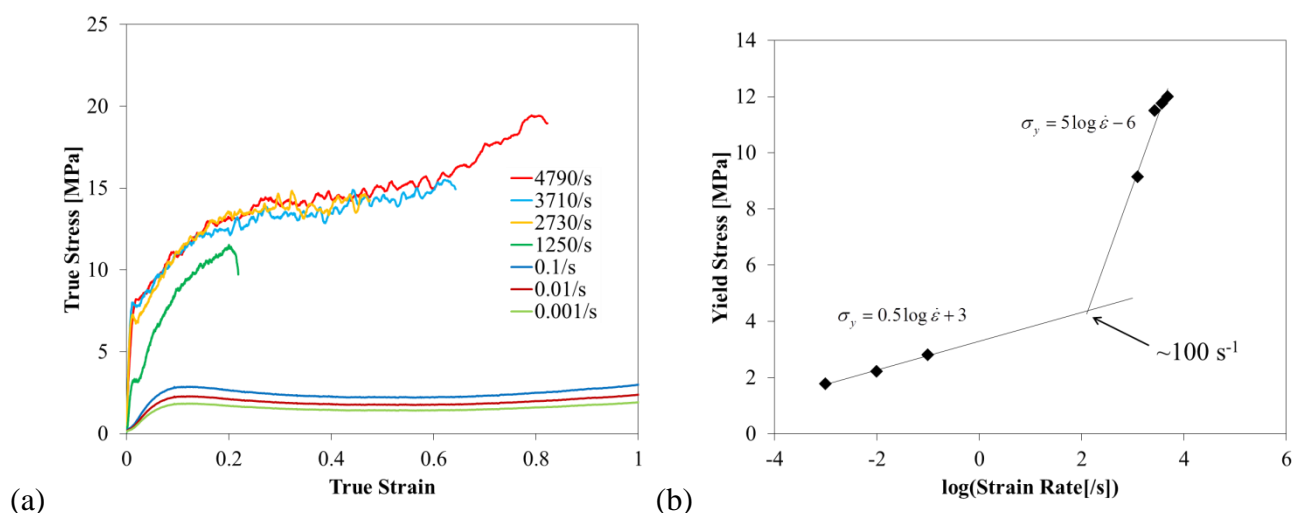
Figure 52. Representative (a) true stress-true strain and (b) yield stress behavior of PBS as a function of strain rate (10^{-3} – 4790 s^{-1}).

Brazilian testing results are summarized in Figure 53, which shows tensile stress against compressive anvil displacement. The high rate behaviour demonstrates an expected (pseudo-)glassy behaviour, due to the system going through its α transition and debonding of the polymer from the matrix, where an increase in strength is observed with increasing strain rate. In the dynamic experiments equilibrium was observed from about 20 μs after the start of testing, which will later be shown to be equivalent to 2% true strain. The temperature dependence agrees with the DMTA data, with no effect above the α transition at about -25 °C.
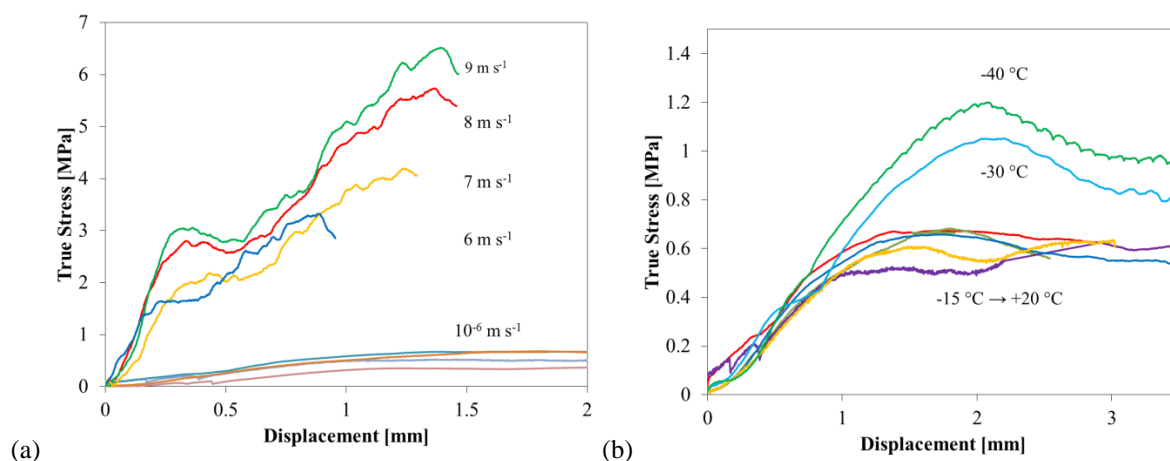
*Figure 53.* Tensile true stress vs compressive displacement response of PBS: dependence on (a) compressive displacement rate and (b) temperature. The 6 m s^{-1} (blue) plot from figure (a) was analysed using DIC to produce true stress-true strain behaviour.

Date	Authors	Page of pages
28 April 2014	CR Siviour, MJ Kendall	64 of 78

The DIC technique was applied to the experiment at 6 m s^{-1} to calculate tensile behaviour, data from the image analysis gave the tensile strain-time curve in Figure 54(a) and hence the tensile stress-strain curve in Figure 54(b). Using the experimental data from this investigation, the experimental simulation method described earlier was extended to capture the high rate behaviour of the PBS in compression and tension.

From the stress-strain data in the high rate experiment, the expected temperature rise under adiabatic loading was calculated, and shown to be very small, less than 1 K. For safety reasons, a low temperature rise during deformation is considered a very desirable characteristic for PBX materials, and it also means that heating can be neglected in the simulation described below.

The two experiments that were simulated were chosen to be at similar strain rates, 1250 s^{-1} in compression and 850 s^{-1} in tension. Hence, in both cases the same test temperature was chosen for the simulation experiments: -45 °C.

The result of simulating the high rate response in compression is presented in Figure 55(a): the simulation captures the high rate behaviour extraordinarily well. Similarly, the tensile data are also well-reproduced by the simulation method, in Figure 55(b). This is an extremely important result: the simulation method is shown to reproduce the high rate behaviour of a polymer bonded explosive simulant in tension, as well as in compression. These results capture a major objective of this project: to predict the high rate behaviour of difficult-to-characterize materials (e.g. composites) via low rate deformation in order to allow for the use of micro-scale imaging tools (e.g. scanning electron microscopes (SEM) and X-ray tomography) to study and better understand these materials' high rate response.

(a)   (b)
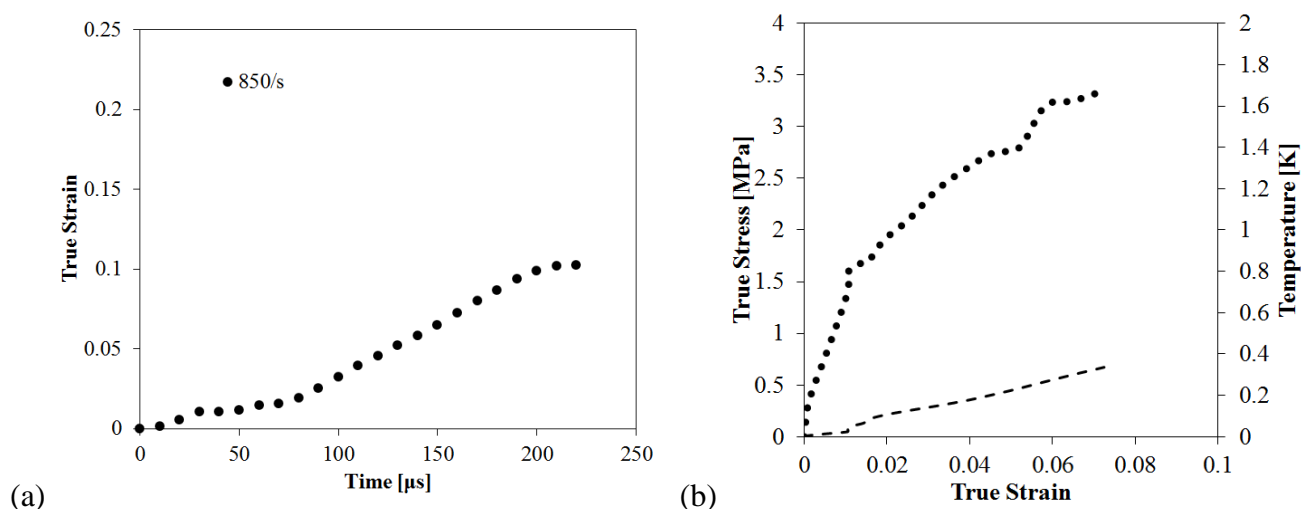
Figure 54. (a) True stain-time curve from Brazilian test, tensile rate is approximately 850 s^{-1}. Each dot on the curve is a true strain value calculated from an image. (b) PBS true stress-true strain behaviour, also shown is the theoretical temperature rise.

Date	Authors	Page of pages
28 April 2014	CR Siviour, MJ Kendall	65 of 78
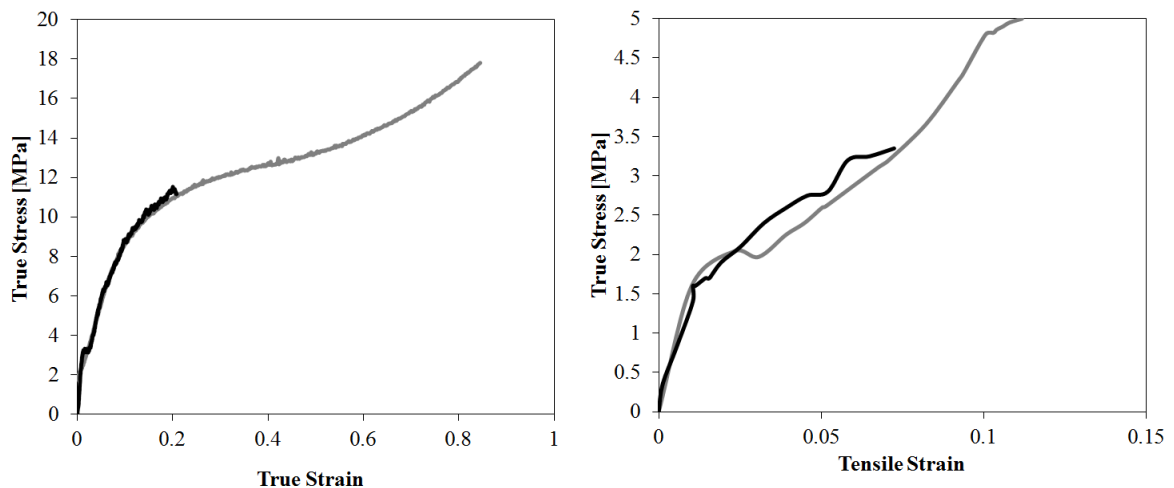
Figure 55. (a) PBS true stress-true strain behaviour in uniaxial compression at 1250 s^{-1} at 20 °C: experiment (black) and experimental simulation (grey) at -45 °C. (b) PBS true stress-true strain behaviour in tension at 850 s^{-1} at 20 °C: experiment (black) and experimental simulation (grey) at 45 °C.

3.6   A novel thermocouple design and further investigations on PVC and PMMA

3.6.1   Background

Much of the previous discussion has been based on the assumption that all of the plastic work done on a specimen is converted into heat and that, furthermore the heat capacity of the material does not change, so that the temperature rise in the specimen can simply be calculated by dividing the work done per unit volume (the integral of the stress-strain curve) by the heat capacity of the specimen. Both of these assumptions may be incorrect: work done can instead increase the internal energy of the specimen through other structural changes, and it is conceivable that the increased mobility of the polymer molecules during plastic deformation may lead to a change in heat capacity, such as occurs at the glass transition. Hence, a number of authors have attempted to measure temperature rises in specimens under high rate deformation, typically using either embedded thermocouples, or infra-red techniques. Results from such measurements indicate that 75 – 100% of the plastic work is converted to heat during moderate to high rate deformation of polymers. This chapter summarises efforts to measure temperature rises in PVC and PMMA during the current project.

Date	Authors	Page of pages
28 April 2014	CR Siviour, MJ Kendall	66 of 78

3.6.2 Temperature rises in PVC – threaded thermocouple.

Very small K-type thermocouples (bead diameter 0.075 mm) were obtained from Omega Engineering, Inc., Stamford, Connecticut, USA, and were attached to a quick response thermocouple amplifier (with a response rate of K μs^{-1}). After careful calibration (calibration factor 0.0113 ± 0.0003 V K^{-1}), these were embedded in a small hole drilled through 20 wt% PPVC specimens, Figure 56. By drilling the hole through the specimen in this way, it was hoped to create a more even stress distribution than the usual arrangement, in which the thermocouple is inserted from one side. Another advantage of this arrangement is that it prevents shorting of the uninsulated thermocouple wires. With practice, it was possible to weld thermocouple junctions with the wires coming out of both sides.

Three types of specimens were tested in a split-Hopkinson bar: three specimens with no hole (undrilled); a specimen with a hole but no thermocouple (drilled only); two specimens with thermocouples. Stress-strain curves are shown in Figure 57, where it is observed that (a) the temperature rise is consistent with a theoretical analysis that assumes most plastic work is converted to heat; and (b) inserting the thermocouples affects the mechanical response.

Figure 56. Threaded Thermocouple
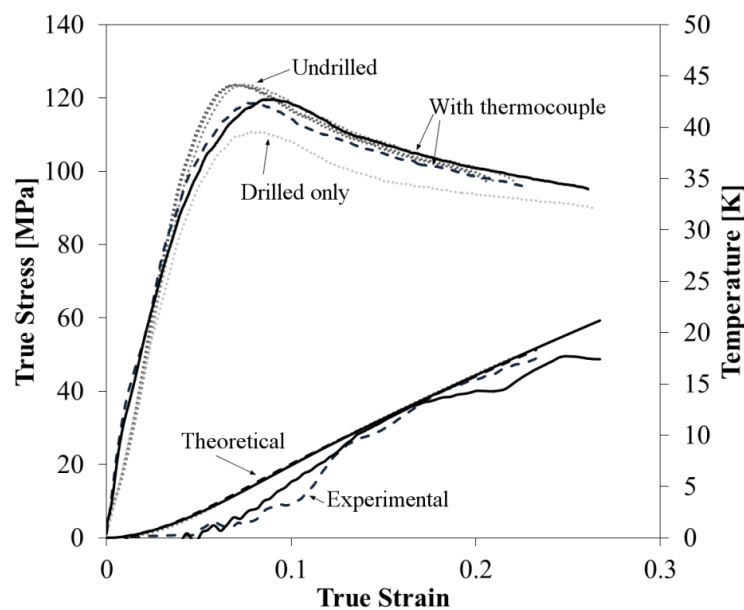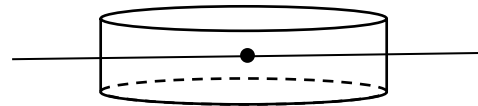
Figure 57. PPVC true stress-true strain behavior and corresponding temperature rise using the threaded method: undrilled specimens tested at 1200 s^{-1}; a drilled specimen with no thermocouple at 1450 s^{-1}; two specimens with thermocouples, at 1250 s^{-1} (black dashed) and 1470 s^{-1} (black solid).

Date	Authors	Page of pages
28 April 2014	CR Siviour, MJ Kendall	67 of 78

3.6.3   Temperature rise in PVC – sandwich thermocouple

In this method, the thermocouple was sandwiched between two specimens, which were joined together with PVC adhesive, Figure 58.   The stress-strain curve obtained with these specimens, Figure 59, shows an improvement over the threaded specimens, especially around the yield stress, although there is still some discrepancy at larger strains.   When performing the experiments, it was observed that whilst the threaded specimens tended to fail around the thermocouple, the sandwich specimens did not, which was consistent with the undrilled response.
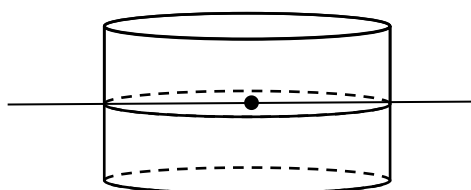
Figure 58. Sandwich thermocouple
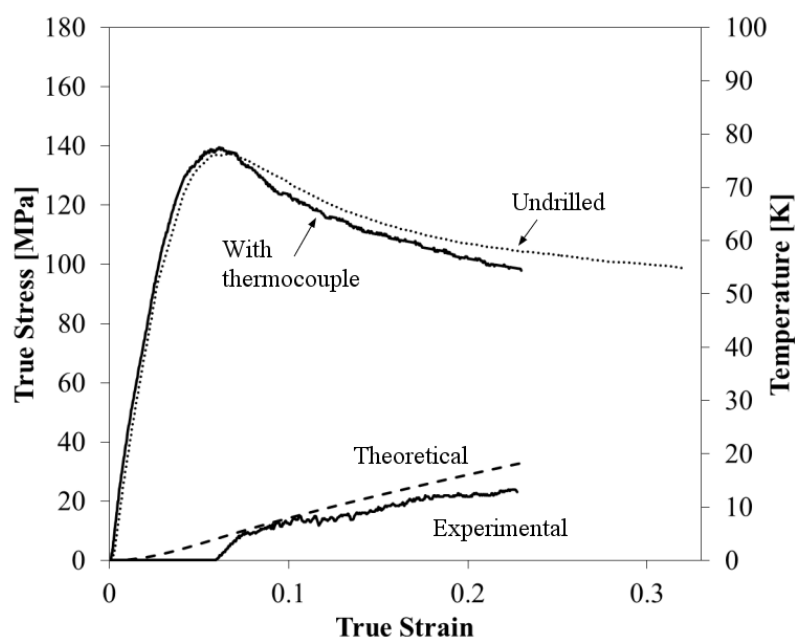
Figure 59. PVC true stress-true strain behaviour using the 'sandwich' method (solid line), and corresponding temperature rises (experimental – solid line; theoretical – dashed line) at 2100 s^{-1}. Representative true stress-true strain behaviour of an undrilled PPVC specimen at 2000 s^{-1} (dotted line) is included for comparison. The rapid increase in temperature near yield is consistent with observations in the literature, e.g. [6].

Date	Authors	Page of pages
28 April 2014	CR Siviour, MJ Kendall	68 of 78

3.6.4 Temperature rise in PMMA – Foil Method

Both the threaded and sandwich methods were found to be unsatisfactory for PMMA, which is significantly less ductile than PVC and therefore more susceptible to the stress concentrations associates with these thermocouples. In order to measure temperature rises whilst maintaining an even stress distribution, a novel sandwich based system was devised, Figure 60, in which the thermocouple is formed by spot-welding two pieces of metal shim. The thermocouple is again sandwiched between two specimens. In this case, copper and constantan shim were used, making a T-type thermocouple.
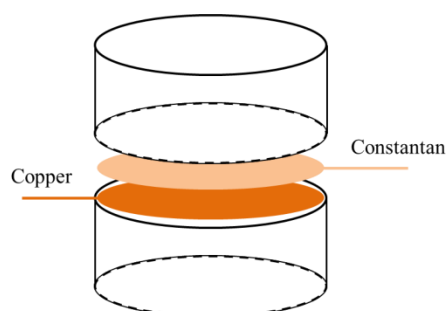
Figure 60. Foil thermocouple

Experimental data from the foil thermocouple are presented in Figure 61, showing that the thermocouple has no observable effect on the behaviour of the specimen. For comparison, data obtained using the threaded method are shown in Figure 62. Not only do the threaded thermocouples interfere more with the specimen response, they also give a lower temperature rise. On examining recovered specimens, brittle failure was observed in the threaded specimens but not in the foil sandwich specimens.

Figure 61. PMMA true stress-true strain behaviour using the foil sandwich method, and corresponding temperature rises (experimental – solid line; theoretical – dashed line) at 0.1 s^{-1}. Representative true stress-true strain behaviours of unmodified PMMA at 0.1 s^{-1} are included for comparison (grey dots).
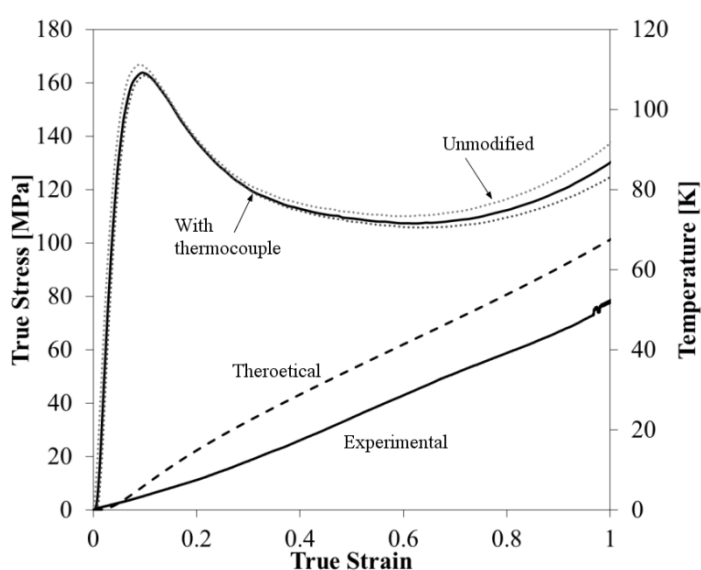
Date	Authors	Page of pages
28 April 2014	CR Siviour, MJ Kendall	69 of 78

Figure 62. PMMA true stress-true strain behaviour and corresponding temperature rise using the threaded method. Stress-strain curves compared for undrilled specimens and a drilled specimen. Theoretical temperature rise compared to experimentally measured temperature rise. Note that a different PMMA material was used in the experiments presented in *Figure* 61 and Figure 62.
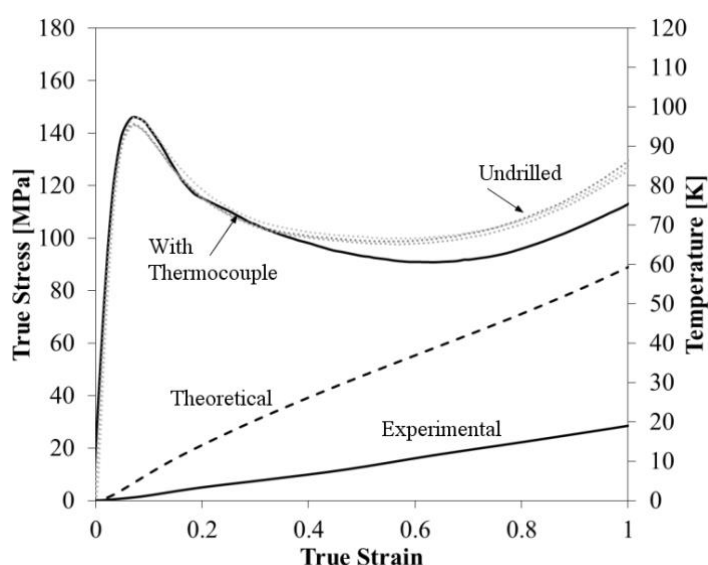
3.6.5   Summary

Three different thermocouple designs were employed to obtain measurements of temperature rises in polymer specimens undergoing plastic deformation. These data were required to support research reported in other parts of the project. In addition to threading thermocouples through the specimens, two sandwich methods were employed, one using a novel foil thermocouple design. This design was found to:

- Give a more accurate temperature measurement than an embedded thermocouple;

- Provide a nearly identical true stress-true strain response to unmodified specimens;

- Avoid pre-mature fracturing seen from embedded thermocouples.

Date	Authors	Page of pages
28 April 2014	CR Siviour, MJ Kendall	70 of 78

4 Conclusions

For PVC materials with different amounts of plasticiser have been extensively characterised, using uniaxial compression tests over a wide range of strain rates and temperatures supported by DMTA experiments. The link between temperature and strain rate dependence in these materials was explored and it was shown again that this link can be described using the frequency dependence of the temperatures at which the α and β transitions occur. The simple linear mapping between strain rate and temperature, previously used by a number of authors, was again applied, using a two process map where required. The mapping parameters obtained by fitting the rate and temperature dependent yield stresses were similar to those obtained by DMTA data, indicating that this procedure has the potential to predict high rate yield stresses using a combination of DMTA and low rate data.

Beyond the yield stress, it was shown that the complete stress-strain response of one of the PVC materials over strain rates from 10^{-3} to 3300 s^{-1} could be replicated in a low strain rate experiment. The yield itself was replicated by reducing the initial temperature of the experiment, whilst the post-yield behaviour was replicated by increasing the temperature during the deformation as if all plastic work done is converted to heat (i.e. β=1), and all heat remains in the specimen. It should be noted that this also makes an assumption about the heat capacity of the material: that it does not change during plastic deformation. All of these assumptions are supported to some extent by temperature measurements made on the material. The straightforward, yet effective approach, offers significant opportunities in better understanding the high rate behavior in a large number of materials. In particular, this technique offers the possibility of better characterizing the behavior of composite materials in which one component is rate sensitive, and to perform experiments on these materials using in-situ diagnostics that cannot be applied to high rate experiments. As well as these immediate opportunities, the simulation of adiabatic conditions as a function of strain offers the potential to develop further insights into the effects of temperature rises in high rate deformation, and highlights the connection between a polymer's temperature-dependent and rate-dependent behavior.

The same method was applied to PMMA and PC. On PMMA, using β=1 gave good simulation of the stress-strain response, but too high a temperature rise. Using the measured value, β=0.75, does not fully capture the post-yield deformation: the simulated stress is too high. Hence, in this material, all of the high rate mechanical work must be replicated by heat in order to replicate the strain softening, indicating softening processes that occur in the higher rate response but are not present at lower rates. In PC, the opposite effect was observed. Although literature data indicate that β is close to 1, only very small temperature rises are required to simulate high rate PC behaviour. The data therefore indicate that there are aspects

Date	Authors	Page of pages
28 April 2014	CR Siviour, MJ Kendall	71 of 78

of the post-yield behaviour for which the interplay between rate and temperature is different from that for the yield stress.

Overall, then, the simulation method is not only able to replicate the high rate behaviour of a number of polymers, with clear advantages for experimental characterisation of composites produced from these polymers, but it is also sensitive enough to show important differences between the expected and observed behaviour. Further work will be required to fully elucidate the microscopic mechanisms responsible for the observed behaviour and to incorporate this into appropriate high rate constitutive models.

Finally, experiments were performed on a particulate composite, a Polymer Bonded Sugar (PBS) with an HTPB binder. Again, a full characterisation was performed under compressive loading supported by DMTA. In addition, indirect tension (Brazilian) tests were performed at low and high strain rates. It was shown that the high rate data could be reproduced by performing quasi-static experiments are reduced temperature. However, in this case, no further temperature profiling was required, as the supported stresses are very low and hence the temperature rises in high rate loading are very small. Further work is therefore required to test this approach on more materials, and also to use the technique with relevant in-situ microscopy.

5   Acknowledgements

Date	Authors	Page of pages
28 April 2014	CR Siviour, MJ Kendall	72 of 78

6 References

1. Field, J.E., et al., *Review of experimental techniques for high rate deformation and shock studies.* International Journal of Impact Engineering, 2004. **30**(7): p. 725-775.

2. Bauwens-Crowet, C., *The compression yield behaviour of polymethyl methacrylate over a wide range of temperatures and strain-rates.* Journal of Materials Science, 1973. **8**(7): p. 968-979.

3. Siviour, C.R., et al., *The high strain rate compressive behaviour of polycarbonate and polyvinylidene difluoride.* Polymer, 2005. **46**(26): p. 12546-12555.

4. Furmanski, J., C.M. Cady, and E.N. Brown, *Time-temperature equivalence and adiabatic heating at large strains in high density polyethylene and ultrahigh molecular weight polyethylene.* Polymer, 2013. **54**(1): p. 381-390.

5. Gerlach, R., et al., *Experimental characterisation and constitutive modelling of RTM-6 resin under impact loading.* Polymer, 2008. **49**(11): p. 2728-2737.

6. Jordan, J.L., J.R. Foley, and C.R. Siviour, *Mechanical properties of Epon 826/DEA epoxy.* Mechanics of Time-Dependent Materials, 2008. **12**(3): p. 249-272.

7. Jordan, J.L., et al., *Compressive properties of extruded polytetrafluoroethylene.* Polymer, 2007. **48**(14): p. 4184-4195.

8. Thompson, D.G., R. DeLuca, and W.J. Wright, *Time-temperature superposition applied to PBX mechanical properties*, in *Shock Compression of Condensed Matter - 2011, Pts 1 and 2*, M.L. Elert, et al., Editors. 2012.

9. Williamson, D.M., et al., *Temperature-time response of a polymer bonded explosive in compression (EDC37).* Journal of Physics D-Applied Physics, 2008. **41**(8).

10. Richeton, J., et al., *Influence of temperature and strain rate on the mechanical behavior of three amorphous polymers: Characterization and modeling of the compressive yield stress.* International Journal of Solids and Structures, 2006. **43**(7-8): p. 2318-2335.

11. Bauwens, J.C., Bauwensc.C, and G. Homes, *Tensile Yield-Stress Behavior of Poly(Vinyl Chloride) and Polycarbonate in Glass Transition Region.* Journal of Polymer Science Part a-2-Polymer Physics, 1969. **7**(10PA): p. 1745-&.

12. Mulliken, A.D. and M.C. Boyce, *Mechanics of the rate-dependent elastic-plastic deformation of glassy polymers from low to high strain rates.* International Journal of Solids and Structures, 2006. **43**(5): p. 1331-1356.

13. Soong, S.Y., et al., *Rate-dependent deformation behavior of POSS-filled and plasticized poly(vinyl chloride).* Macromolecules, 2006. **39**(8): p. 2900-2908.

14. Walley, S. and J. Field, *Strain rate sensitivity of polymers in compression from low to high rates.* Dymat Journal, 1994. **1**: p. 211-228.

15. Kolsky, H., *An investigation of the mechanical properties of materials at very high rates of loading.* Proc. Phys. Soc. Lond. B, 1949. **62**: p. 676-700.

Date	Authors	Page of pages
28 April 2014	CR Siviour, MJ Kendall	73 of 78

16. Chou, S.C., K.D. Robertson, and J.H. Rainey, *Effect of strain rate and heat developed during deformation on stres-strain curves of plastics.* Experimental Mechanics, 1973. **13**(10): p. 422-432.

17. Rietsch, F. and B. Bouette, *The Compression Yield Behavior of Polycarbonate over a Wide-Range of Strain Rates and Temperatures.* European Polymer Journal, 1990. **26**(10): p. 1071-1075.

18. Al-Maliky, N., et al., *Drops in the flow stress of semi-crystalline polymers at very high rates of strain.* Journal of Materials Science Letters, 1998. **17**(13): p. 1141-1143.

19. Hamdan, S. and G.M. Swallowe, *The strain-rate and temperature dependence of the mechanical properties of polyetherketone and polyetheretherketone.* Journal of Materials Science, 1996. **31**(6): p. 1415-1423.

20. Dioh, N.N., et al., *The High-Strain Rate Behavior of Polymers.* Journal De Physique Iv, 1994. **4**(C8): p. 119-124.

21. Dioh, N.N., P.S. Leevers, and J.G. Williams, *Thickness Effects in Split Hopkinson Pressure Bar Tests.* Polymer, 1993. **34**(20): p. 4230-4234.

22. Cady, C.M., et al., *Determining the constitutive response of polymeric materials as a function of temperature and strain rate.* Journal De Physique Iv, 2003. **110**: p. 27-32.

23. Brown, E.N., et al., *Influence of molecular conformation on the constitutive response of polyethylene: A comparison of HDPE, UHMWPE, and PEX.* Experimental Mechanics, 2007. **47**(3): p. 381-393.

24. Arruda, E.M., M.C. Boyce, and R. Jayachandran, *Effects of strain-rate, temperature and thermomechanical coupling on the finite strain deformation of glassy-polymers.* Mechanics of Materials, 1995. **19**(2-3): p. 193-212.

25. Rittel, D., *On the conversion of plastic work to heat during high strain rate deformation of glassy polymers.* Mechanics of Materials, 1999. **31**(2): p. 131-139.

26. Regev, A. and D. Rittel, *Simultaneous transient temperature sensing of impacted polymers using infrared detectors and thermocouples.* Experimental Mechanics, 2008. **48**(5): p. 675-682.

27. Garg, M., A.D. Mulliken, and M.C. Boyce, *Temperature rise in polymeric materials during high rate deformation.* Journal of Applied Mechanics-Transactions of the Asme, 2008. **75**(1).

28. Hillmansen, S. and R.N. Haward, *Adiabatic failure in polyethylene.* Polymer, 2001. **42**(22): p. 9301-9312.

29. Hillmansen, S., et al., *The effect of strain rate, temperature, and molecular mass on the tensile deformation of polyethylene.* Polymer Engineering and Science, 2000. **40**(2): p. 481-489.

30. Gray III, G., *Classic split-Hopkinson pressure bar testing*, in *ASM Handbook Vol. 8: Mechanical Testing and Evaluation*, D. Medlin, Editor. 2000, ASM International. p. 488-496.

Date	Authors	Page of pages
28 April 2014	CR Siviour, MJ Kendall	74 of 78

31.   Roland, C.M., et al., *Mechanical response of rubber at high strain rates.* Abstracts of Papers of the American Chemical Society, 2007. **234**.

32.   Song, B., et al., *A Long Split Hopkinson Pressure Bar (LSHPB) for Intermediate-rate Characterization of Soft Materials.* Experimental Mechanics, 2008. **48**(6): p. 809-815.

33.   Cloete, T.J. and S. Oxtoby, *A new technique for compression tests at intermediate strain rates: Prototype results.* Dymat 2009: 9th International Conference on the Mechanical and Physical Behaviour of Materials under Dynamic Loading, Vol 1, 2009: p. 249-255.

34.   Hockett, J.E. and N.A. Lindsay, *Cam Plastometer Data Acquistition System.* Journal of Physics E-Scientific Instruments, 1971. **4**(7): p. 520-&.

35.   Baragar, D.L., *The High-Temperature and High Strain-Rate Behavior of a Plain Carbon and an Hsla Steel.* Journal of Mechanical Working Technology, 1987. **14**(3): p. 295-307.

36.   Foot, J.S., et al., *The Yield Behavior of Amorphous Polyethylene Terephthalate - an Activated Rate Theory Approach.* Journal of Materials Science, 1987. **22**(4): p. 1437-1442.

37.   Cai, J., et al., *High-strain, high-strain-rate flow and failure in PTFE/Al/W granular composites.* Materials Science and Engineering a-Structural Materials Properties Microstructure and Processing, 2008. **472**(1-2): p. 308-315.

38.   Gray III, G.T., *Classic split-Hopkinson pressure bar testing*, in *ASM Handbook. Vol. 8: Mechanical Testing and Evaluation*, H. Kuhn and D. Medlin, Editors. 2000, ASM International: Materials Park, Ohio. p. 462-476.

39.   Gray III, G.T. and W.R. Blumenthal, *Split-Hopkinson pressure bar testing of soft materials*, in *ASM Handbook. Vol. 8: Mechanical Testing and Evaluation*, H. Kuhn and D. Medlin, Editors. 2000, ASM International: Materials Park, Ohio. p. 488-496.

40.   Li, P., C.R. Siviour, and N. Petrinic, *The Effect of Strain Rate, Specimen Geometry and Lubrication on Responses of Aluminium AA2024 in Uniaxial Compression Experiments.* Experimental Mechanics, 2009. **49**(4): p. 587-593.

41.   Gorham, D.A., *The effect of specimen dimension on high-strain rate compression measurements of copper.* Journal of Physics D-Applied Physics, 1991. **24**(8): p. 1489-1492.

42.   Trautmann, A., et al., *Lubrication of polycarbonate at cryogenic temperatures in the split Hopkinson pressure bar.* International Journal of Impact Engineering, 2005. **31**(5): p. 523-544.

43.   Okereke, M.I., C.P. Buckley, and C.R. Siviour, *Compression of polypropylene across a wide range of strain rates.* Mechanics of Time-Dependent Materials, 2012. **16**(4): p. 361-379.

44.   Rae, P.J., et al., *Quasi-static studies of the deformation and failure of beta-HMX based polymer bonded explosives.* Proceedings of the Royal Society a-Mathematical Physical and Engineering Sciences, 2002. **458**(2019): p. 743-762.

Date	Authors	Page of pages
28 April 2014	CR Siviour, MJ Kendall	75 of 78

45. Awaji, H. and S. Sato, *Diametral Compressive Testing Method.* Journal of Engineering Materials and Technology-Transactions of the Asme, 1979. **101**(2): p. 139-147.

46. Grantham, S.G., et al., *High-strain rate Brazilian testing of an explosive simulant using speckle metrology.* Measurement Science & Technology, 2004. **15**(9): p. 1867-1870.

47. Rae, P.J., et al., *White-light digital image cross-correlation (DICC) analysis of the deformation of composite materials with random microstructure.* Optics and Lasers in Engineering, 2004. **41**(4): p. 635-648.

48. Titow, W.V., *PVC Technology.* 1984: Springer.

49. Davies, E.D.H. and S.C. Hunter, *The Dynamic Compression Testing of Solids by the Method of the Split Hopkinson Pressure Bar.* Journal of the Mechanics and Physics of Solids, 1963. **11**(3): p. 155-179.

50. Wang, Y., E.M. Arruda, and P.A. Przybylo, *Characterization and constitutive modeling of a plasticized poly(vinyl chloride) for a broad range of strain rates.* Rubber Chemistry and Technology, 2001. **74**(4): p. 560-573.

51. Matthews, G., *Properties of vinyl chloride polymers and copolymers*, in *PVC: Production, Properties, and Uses.* 1996, Institute of Materials: London.

52. Hasan, O.A., et al., *An Investigation of the Yield and Post-Yield Behavior and Corresponding Structure of Poly(Methyl Methacrylate).* Journal of Polymer Science Part B-Polymer Physics, 1993. **31**(2): p. 185-197.

53. Lee, S.F. and G.M. Swallowe, *Quasi-static and dynamic compressive behaviour of poly(methyl methacrylate) and polystyrene at temperatures from 293 K to 363 K.* Journal of Materials Science, 2006. **41**(19): p. 6280-6289.

54. Rittel, D. and A. Brill, *Dynamic flow and failure of confined polymethylmethacrylate.* Journal of the Mechanics and Physics of Solids, 2008. **56**(4): p. 1401-1416.

55. Lerch, V., G. Gary, and P. Herve, *Thermomechanical properties of polycarbonate under dynamic loading.* Journal De Physique Iv, 2003. **110**: p. 159-164.

56. Li, Z.H. and J. Lambros, *Strain rate effects on the thermomechanical behavior of polymers.* International Journal of Solids and Structures, 2001. **38**(20): p. 3549-3562.

57. Mulliken, A., *Mechanics of amorphous polymers and polymer nanocomposites during high rate deformation*, in *Mechanical Engineering.* 2006, Massachusetts Institute of Technology.

58. Bauwens, J.C., *Relation between compression yield stres and mechanical loss peak of Bysphenol-A-Polycarbonate in beta-transition range.* Journal of Materials Science, 1972. **7**(5): p. 577-&.

59. Rudnev, S.N., et al., *Plastic-deformation kinetics for glassy-polymers and blends.* Colloid and Polymer Science, 1991. **269**(5): p. 460-468.

60. Boyce, M. and R. Haward, *The post yield deformation of glass polymers*, in *The Physics of Glassy Polymers*, R.N. Haward and R.J. Young, Editors. 1997, Chapman and Hall: London. p. 508.

Date	Authors	Page of pages
28 April 2014	CR Siviour, MJ Kendall	76 of 78

61. Palmer, S.J.P., J.E. Field, and J.M. Huntley, *Deformation, strengths and strains to failure of polymer bonded explosives.* Proc. R. Soc. Lond. A, 1993. **440**: p. 399-419.

62. Walley, S.M., et al., *High-Rate Mechanical Properties of Energetic Materials.* Jom, 2010. **62**(1): p. 31-34.

63. Bowden, F.P. and A.D. Yoffe, *Initiation and Growth of Explosion in Liquids and Solids (republ. 1985).* 1952, Cambridge: Cambridge University Press.

64. Bowden, F.P. and A.D. Yoffe, *Fast Reactions in Solids.* 1958, London: Butterworth.

65. Field, J.E., et al., *Hot-spot ignition mechanisms for explosives and propellants.* Phil. Trans. R. Soc. Lond. A, 1992. **339**: p. 269-283.

66. Ho, S.Y., *Impact ignition mechanisms of rocket propellants.* Combustion & Flame, 1992. **91**: p. 131-142.

67. Ho, S.Y., *High strain-rate impact ignition of rocket propellants*, in *Proc. 10th Int. Detonation Symposium*, J.M. Short and D.G. Tasker, Editors. 1995, Office of Naval Research: Arlington, Virginia. p. 94-103.

68. Walley, S.M., J.E. Field, and S.J.P. Palmer, *Impact sensitivity of propellants.* Proc. R. Soc. Lond. A, 1992. **438**: p. 571-583.

69. Ho, S.Y. and C.W. Fong, *Relationship between impact ignition sensitivity and kinetics of the thermal decomposition of solid propellants.* Combustion & Flame, 1989. **75**: p. 139-151.

70. Swallowe, G.M. and J.E. Field, *The ignition of a thin layer of explosive by impact: The effect of polymer particles.* Proc. R. Soc. Lond. A, 1982. **379**: p. 389-408.

71. Williamson, D.M., et al., *Brazilian Disc Testing of a Uk Pbx Approaching the Glass Transition Condition.* Shock Compression of Condensed Matter - 2009, Pts 1 and 2, 2009. **1195**: p. 494-497.

72. Balzer, J.E., et al., *High-speed photographic study of the drop-weight impact response of ultrafine and conventional PETN and RDX.* Combust. Flame, 2002. **130**: p. 298-306.

73. Balzer, J.E., et al., *Behaviour of ammonium perchlorate-based propellants and a polymer-bonded explosive under impact loading.* Proc. R. Soc. Lond. A, 2004. **460**: p. 781-806.

74. Gray III, G.T., et al., *Influence of temperature on the high strain-rate mechanical behavior of PBX 9501*, in *Shock Compression of Condensed Matter - 1997*, S.C. Schmidt, D.P. Dandekar, and J.W. Forbes, Editors. 1998, American Institute of Physics: Woodbury, New York. p. 583-586.

75. Gray III, G.T., et al., *High- and low-strain rate compression properties of several energetic material composites as a function of strain rate and temperature*, in *Proc. 11th Int. Detonation Symposium*, J.M. Short and J.E. Kennedy, Editors. 2000, Office of Naval Research: Arlington, Virginia. p. 76-84.

76. Williamson, D., et al., *Mechanical properties of PBS9501*, in *Shock Compression of Condensed Matter - 2003*, M.D. Furnish, Y.M. Gupta, and J.W. Forbes, Editors. 2004, American Institute of Physics: Melville NY. p. 816-819.

77. Drodge, D.R., et al., *Hopkinson bar studies of a PBX simulant.* Shock Compression of Condensed Matter - 2007, Pts 1 and 2, 2007. **955**: p. 513-516.

78. Drodge, D.R., et al., *Strain-Rate Master Curves for a Pbx and Binder.* Shock Compression of Condensed Matter - 2011, Pts 1 and 2, 2012. **1426**.

79. Drodge, D.R., et al., *The mechanical response of a PBX and binder: combining results across the strain-rate and frequency domains.* Journal of Physics D-Applied Physics, 2010. **43**(33).

80. Siviour, C.R., et al., *High strain rate properties of a polymer-bonded sugar: their dependence on applied and internal constraints.* Proceedings of the Royal Society a-Mathematical Physical and Engineering Sciences, 2008. **464**(2093): p. 1229-1255.